Arch. Mech., 44, 5, pp. 621–662, Warszawa 1992

Some remarks on macroscopic observations and related microscopic phenomena of the mechanical behaviour of metallic materials

B. WACK and A. TOURABI (GRENOBLE)

ON THE BASIS of some experimental macroscopic results a qualitative correspondence may be established between the macroscopic hysteresis behaviour and the microstructural phenomena which are responsible for the deformation.

1. Introduction

THE PRESENT PAPER is an attempt to bring nearer two different approaches to deformation: the macroscopic approach of continuum mechanics, through phenomenological descriptions of the behaviour, which often ignores the detailed microscopic mechanisms of deformation (and their possible consequences on the macroscopic behaviour) and the physical microscopic investigation of the operation of these mechanisms, which cannot be easily generalized to account for the three-dimensional macroscopic properties. Since this paper is intended for both mechanicians and physical metallurgists it has been purposely written in a circumstantial way, which could seem overdetailed to some readers belonging to either community, to whom the authors would like to apologize.

The behaviour of metallic materials may be considered as reversible when the load amplitude and the number of load cycles are small enough; the multitude of applications designed and built by engineers shows that this simplification is largely justified in that case. But we know, through accurate observations, that crystalline materials and particularly metallic materials never behave exactly as an elastic continuum even in this case; for example, it is always possible to break a sample under a cyclic loading of small amplitude if the number of cycles is great enough([1]).

It seems that only two extreme cases exist where metallic materials may behave strictly as elastic materials. The first case is a state of crystalline structure without any defect in the bulk: one may obtain this state only under the form of whiskers [7]. We also notice that these materials are the only ones for which the mechanical properties are very close to the values deduced theoretically from the perfect crystalline structure. The other case, where an elastic behaviour domain exists, is represented by the piano wire and other wires obtained by similar processes. For these materials the dislocation density is so high and the dislocations are so entangled that a very large stress is necessary to unpin dislocations; this probably explains why for these materials also second-order effects, like-Poynting effect [8, 9], are reversible.

The aim of this paper is to discuss the validity of the basic assumptions of a constitutive scheme established at a macroscopic scale [10÷15], with the help of the analysis of related

([1]) As analysed by BELL [1], some related macroscopic experimental results were obtained a long time ago [2, 3, 4]. More recently material physicists also noticed irreversible deformation at very low stresses [5, 6].

phenomena at a microscopic scale. For that purpose we first present some experimental macroscopic results which bring to evidence the properties of the mechanical hysteresis behaviour (Sec. 2). Secondly we try to find at a microstructural scale the explanation and the justification of this mechanical hysteresis behaviour: on the basis of a few examples of elementary microstructural mechanisms of deformation, at the scale of dislocations motion (Sec. 3), it is shown that a great variety of such elementary microstructural mechanisms may be symbolically represented by a continuous distribution of spring and friction slider couples (Sec. 4). Since this symbolic representation is the same as the one used to build the macroscopic behaviour description, a qualitative correspondence may be established between the macroscopic behaviour of crystalline materials and the microstructural phenomena which control the deformation of these materials. This qualitative correspondence sheds a new light on classical notions like the separation of the total strain into an elastic and a plastic one, the local internal stress, the separation between low cycle fatigue and high cycle fatigue, etc. (Sec. 5). Finally the relative importance of viscosity and pure hysteresis is discussed (Sec. 6).

2. Experimental macroscopic results

2.1. Experimental procedure

For metallic materials the hysteresis contribution of the behaviour never exists alone and is generally accompanied by other phenomena like hardening, softening, viscosity. In order to identify and quantify the hysteresis contribution some particular precautions have to be taken. First for each given strain amplitude a sufficient number of symmetrical cycles are carried out in order to obtain a stabilized cycle, and thus to strongly reduce the influence of hardening (or softening).

Secondly all the tests are carried out at room temperature, which can be considered as a low temperature for the materials studied here ($T/T_m < 0.3$) and at a constant and low strain rate in order to minimize the influence of viscosity (cf. Sec. 6).

In order to give a larger validity to the conclusions of this study, a series of five typical metallic materials is studied:

- as received cold drawn copper,
- commercial brass (58.10 wt % Cu; 38.53 wt % Zn; 3.20 wt % Pb),
- engineering steel (0.97 wt % Cr; 0.60 wt % Mn; 0.38 wt % C),
- stainless steel (17.93 wt % Cr; 12.48 wt % Ni; 2.40 wt % Mo),
- duralumin (3.80 wt % Cu).

Furthermore the unidirectional loadings are of two types: tension-compression or simple torsion. For all the tests the sample has a tubular shape with, typically, an external radius of 15 mm and an internal radius of 12 mm. The axial and shear strains are measured locally with an extensometer. In order to reduce the error due to the inhomogeneity of the stress and strain through the tube thickness for the torsion test, the stress-strain curve is determined for the mean radius. All the tests are controlled at a constant strain rate of about 10^{-4} s^{-1}; this value is a good compromise between the reduction of the influence of the viscosity effects and the test duration [18].

2.2. The restorable neutral state

The mechanical hysteresis contribution of the behaviour exhibits a neutral state which may be restored after any strain history. The restoration is obtained first with a loading of sufficiently large amplitude, so as to reach the first loading curve and thus to erase the memory of the preceding loadings, and secondly by the "fundamental cyclic test", defined as a quasi-symmetrical cyclic test of slowly decreasing strain amplitude, similar to the demagnetization process of ferro-magnetic materials. This notion of neutral state is illustrated by the following two examples.

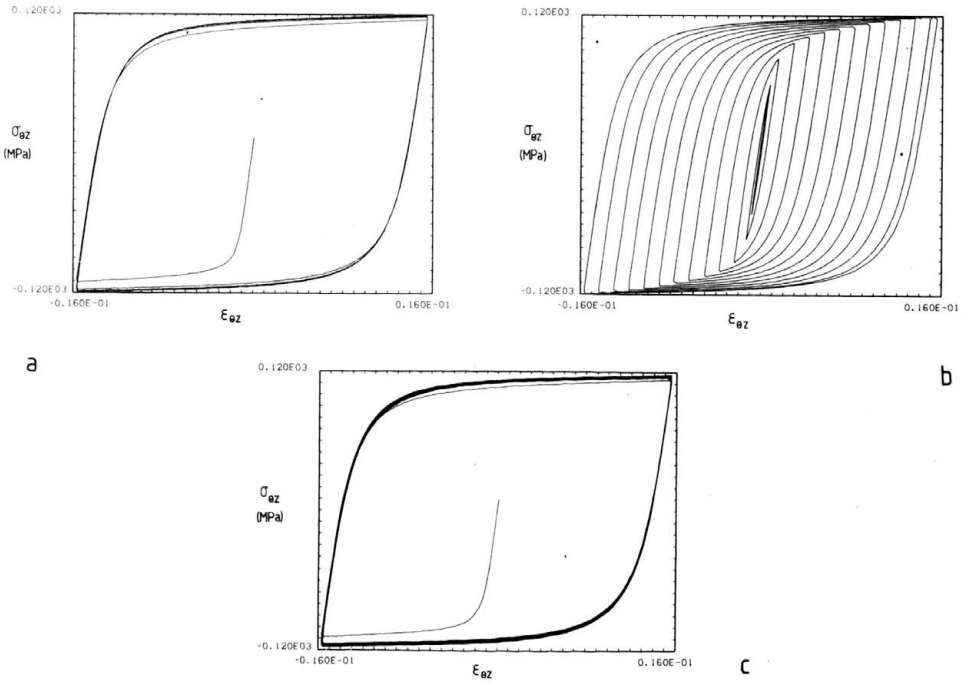

FIG. 1. Cyclic torsion test. Cold drawn copper (test 501): a) first reloading; b) second fundamental cyclic test; c) second reloading.

The first example concerns as received cold drawn copper. The test is a cyclic torsion test, strain controlled at $\pm 1.5\%$. The preliminary step consists first of a sufficient number of cycles to reach a quasi-stabilized state which exhibits softening, and secondly of a fundamental cyclic test to restore the presumed neutral state. The test itself consists of a reloading followed by a few cycles, a fundamental cyclic test and finally a second reloading followed by a few cycles (Fig. 1a, b and c). The identity of the results before (Fig. 1a) and after (Fig. 1c) the fundamental cyclic test validates the notion of restorable neutral state.

The second example concerns a commercial brass in a simple torsion test. After a few dozens of cycles of different amplitudes, a fundamental cyclic test was conducted to erase the memory of the preceding inversion states and to restore the neutral state (Fig. 2a). Then the same steps were repeated: reloading to a strain of 1.5% followed by a

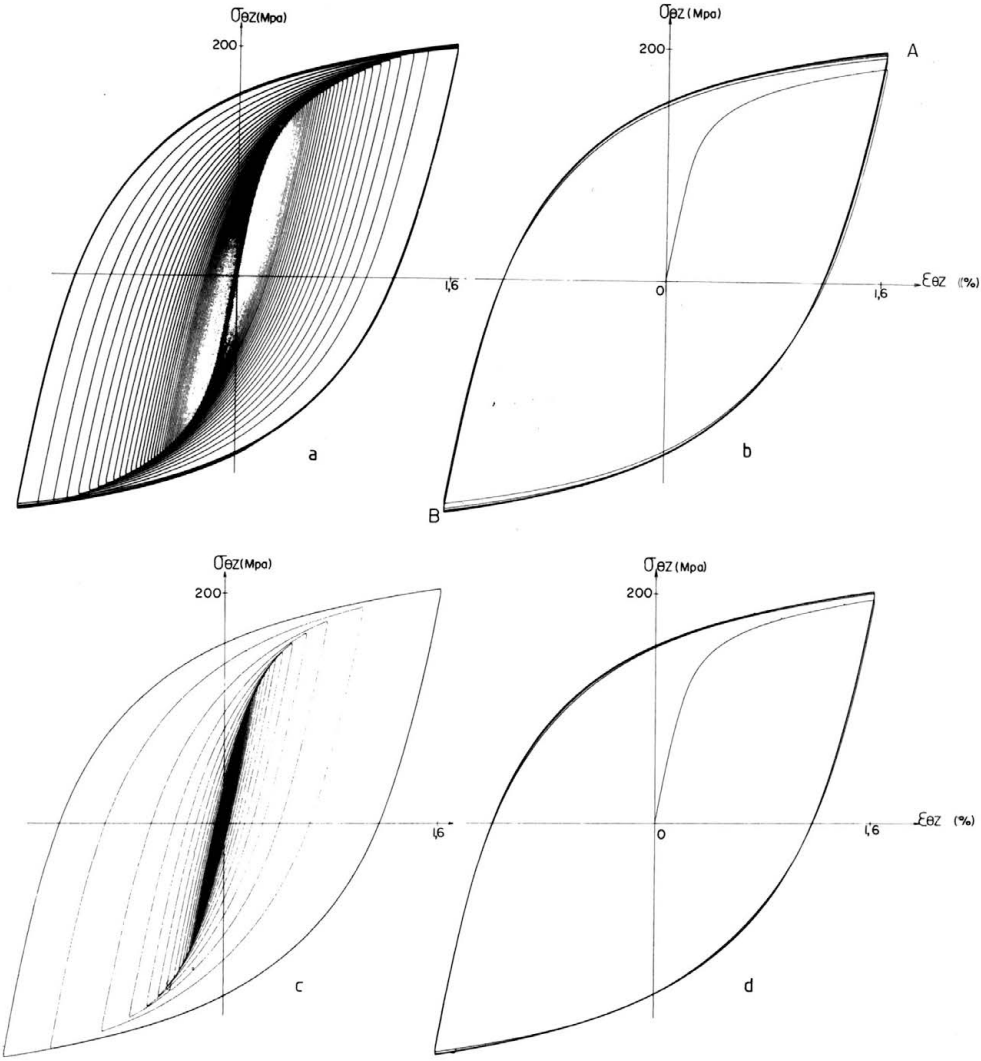

FIG. 2. Cyclic torsion test. Commercial brass (test 603): a) first fundamental cyclic test; b) first reloading; c) second fundamental cyclic test; d) second reloading.

few symmetrical cycles (Fig. 2b), a fundamental cyclic test (Fig. 2c) and finally a second reloading (Fig. 2d). The two reloadings (Fig. 2b and d) are identical with the exception of the hardening effect, which stays more permanent after the last fundamental cyclic test.

2.3. Loading branches passing through the origin

Another manifestation of the mechanical hysteresis properties concerns the existence of different types of stress-strain curves passing through the origin. They are made obvious from a symmetrical cyclic test $\pm\varepsilon_1$. Four different curves may be defined, as modelized

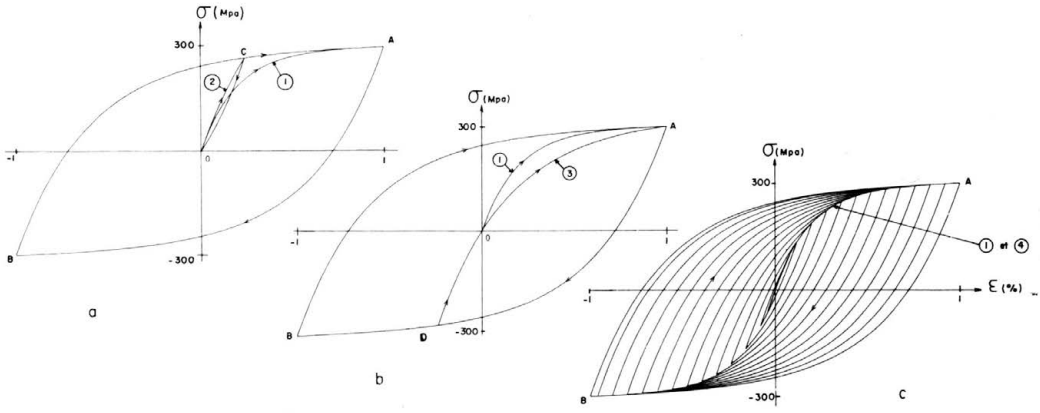

FIG. 3. The definition of the different loading branches passing through the origin.

on Fig. 3, where curve (*1*) is used as reference (see Sec. A.3):

curve (*1*) is the first loading branch,

curve (*2*) is obtained (after an inversion at C chosen so that the unloading branch reaches the origin) by an inversion and a reloading at the origin,

curve (*3*) is obtained by an inversion at D, so that the reloading branch reaches the origin and continues to load in the same direction,

curve (*4*) is the locus of the inversion points of a fundamental cyclic test.

According to the pure hysteresis model curve (*4*) is identical to the first loading branch. The branches AB (or BA) are similar to the first loading branch OA (*1*) with a ratio of 2. The branch OCA is constituted of two arcs; the reference state (as defined later in appendix) is O for the arc OC (*2*) and B for the arc CA. The curve OA (*3*) (Fig. 3b) is the upper part of the loading branch DA, which has its reference state in D and is similar to the beginning of branch BA.

The experimental determination of these curves is made in a global test constituted by four steps, each corresponding to one curve. The steps are preceded by a group of large cycles $\pm\varepsilon_1$ in order to stabilize the hardening (or softening) phenomenon. Furthermore curve (*1*) is determined after a fundamental cyclic test; thus curve (*1*) is not strictly a first loading branch, but it may be considered as equivalent to a first loading branch of a stabilized material as shown previously. The results of six *pure hysteresis global tests* are shown in Figs. 4 to 9: the figures labelled *a* give the details of the four steps and the figures labelled *b* compare the four curves; the fundamental cyclic test made before the first step is not represented.

In spite of the precautions taken, the tests continue to show a slight influence of hardening. This is evidenced by the difference of the ends of the four curves at point A; nevertheless these differences remain small. Two tests are simple tension-compression tests (engineering steel and cold-drawn copper) and four are simple cyclic torsion tests (engineering steel, stainless steel, duralumin and brass). For all tests, curve (*4*) is almost identical to curve (*1*). The difference between the two curves is noticeable essentially at the end of the curves, on the plateau of "quasi-plasticity"; for brass (Fig. 9) this difference

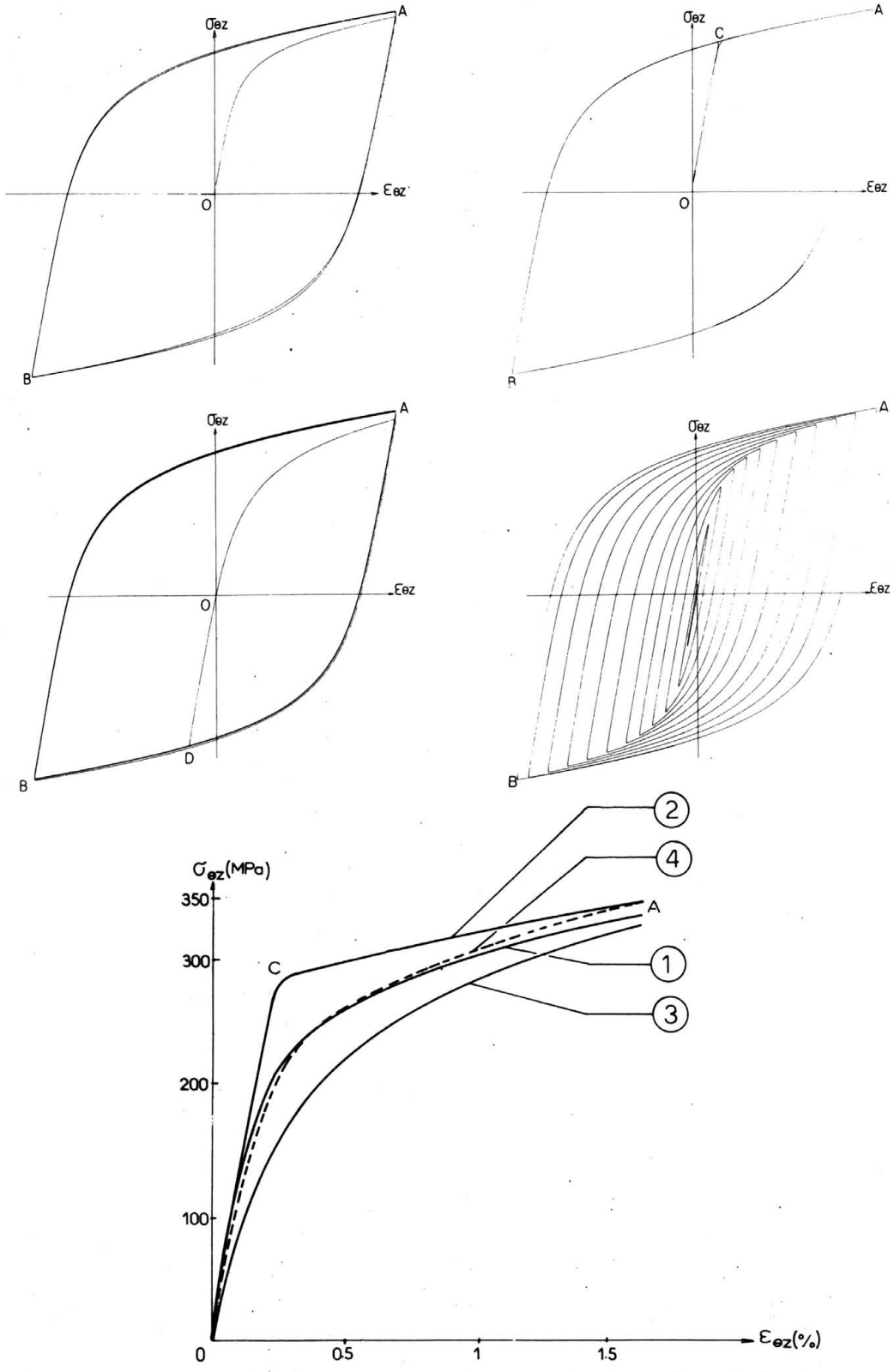

FIG. 4. Loading branches passing through the origin. Cyclic torsion. Engineering steel (test 406).

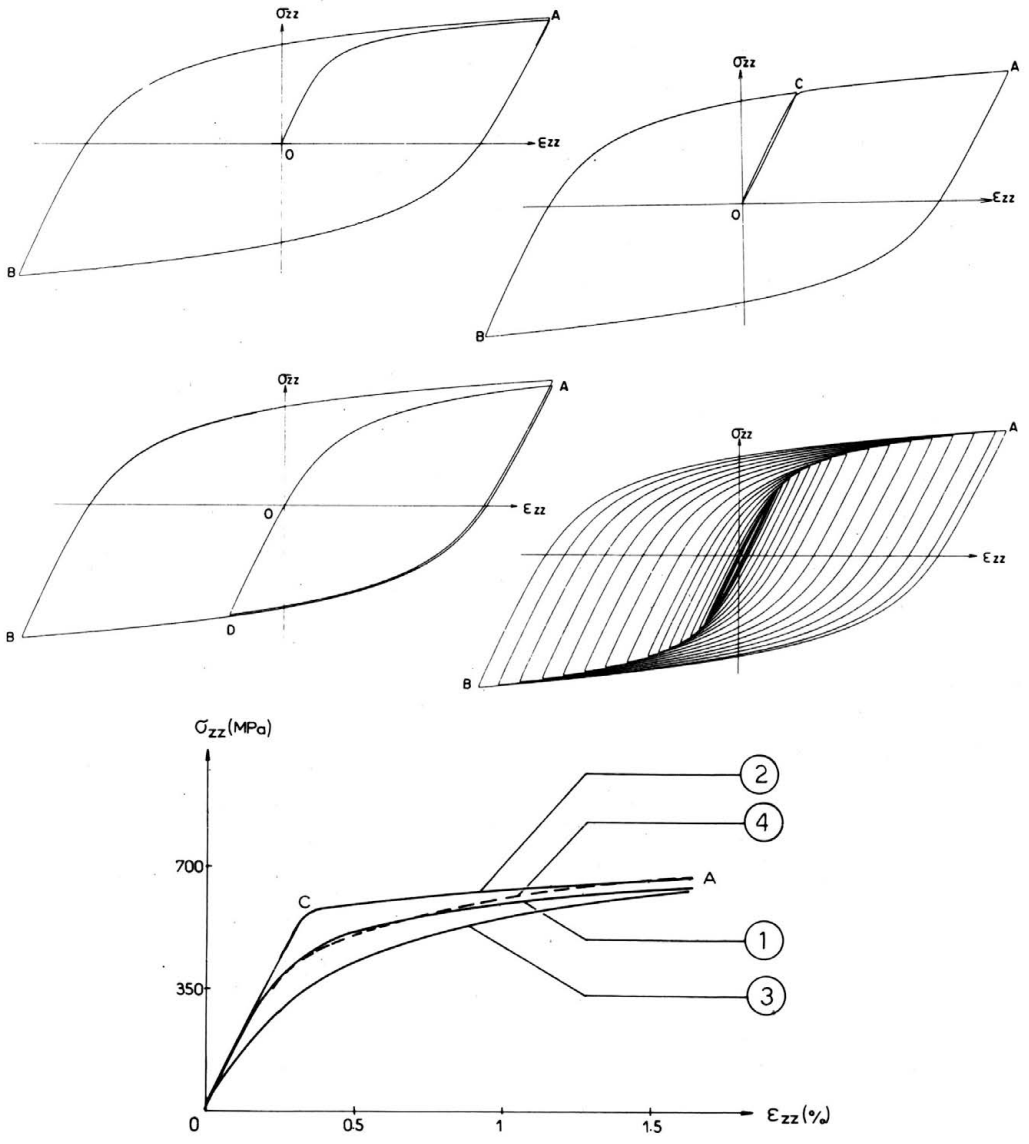

FIG. 5. Loading branches passing through the origin. Cyclic tension-compression. Engineering steel (test 414).

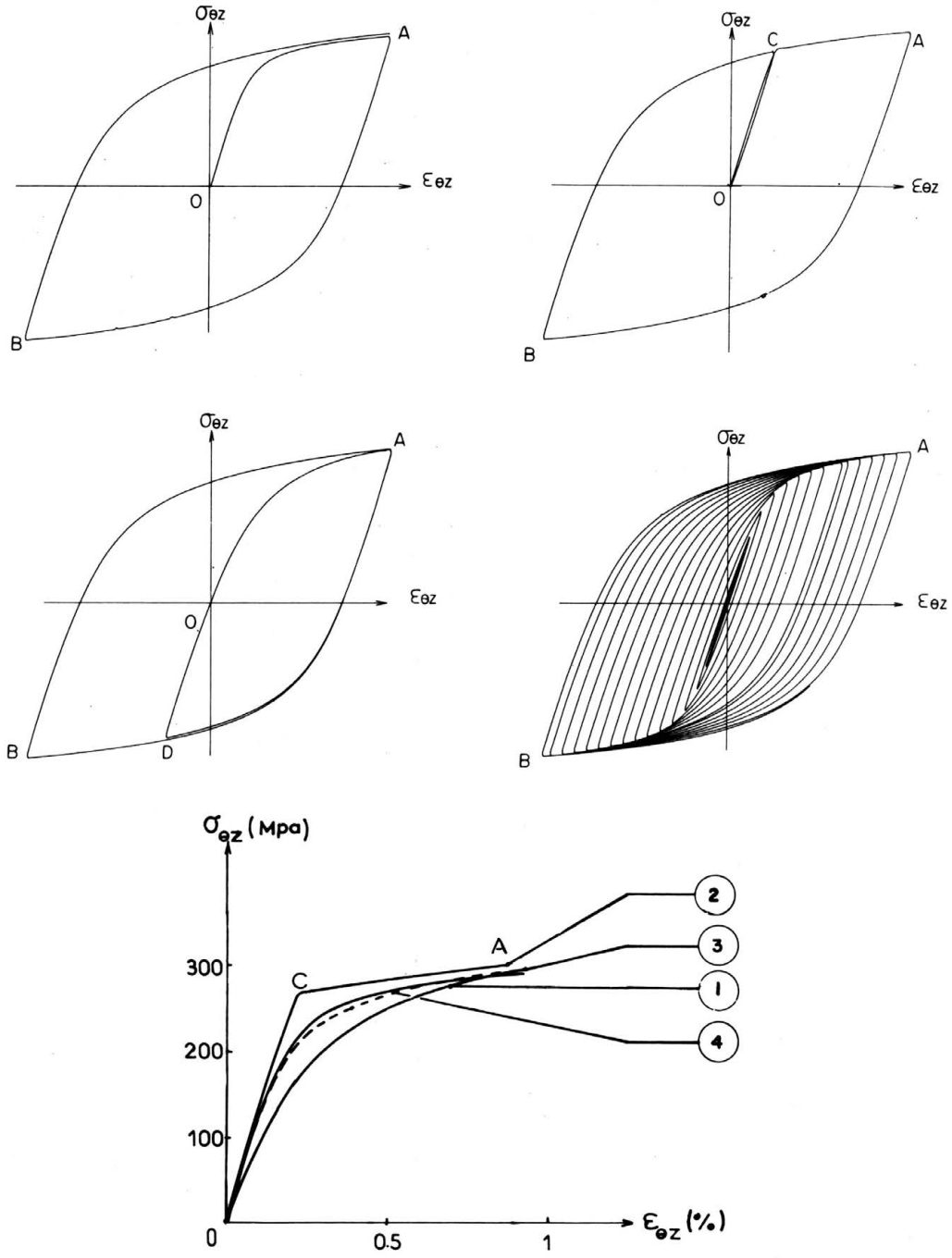

FIG. 6. Loading branches passing through the origin. Cyclic torsion. Stainless steel (test 208).

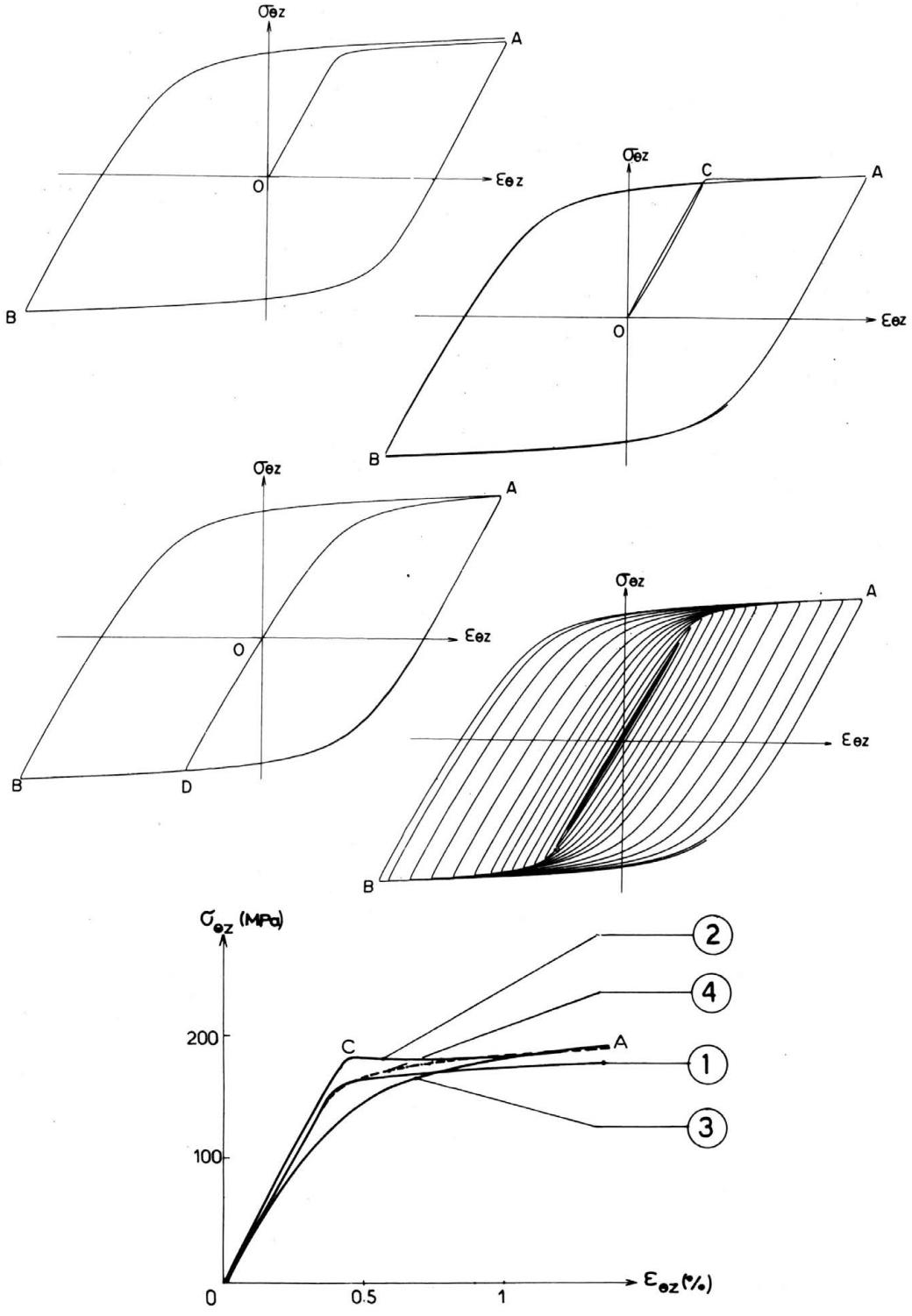

FIG. 7. Loading branches passing through the origin. Cyclic torsion. Duralumin (test 703).

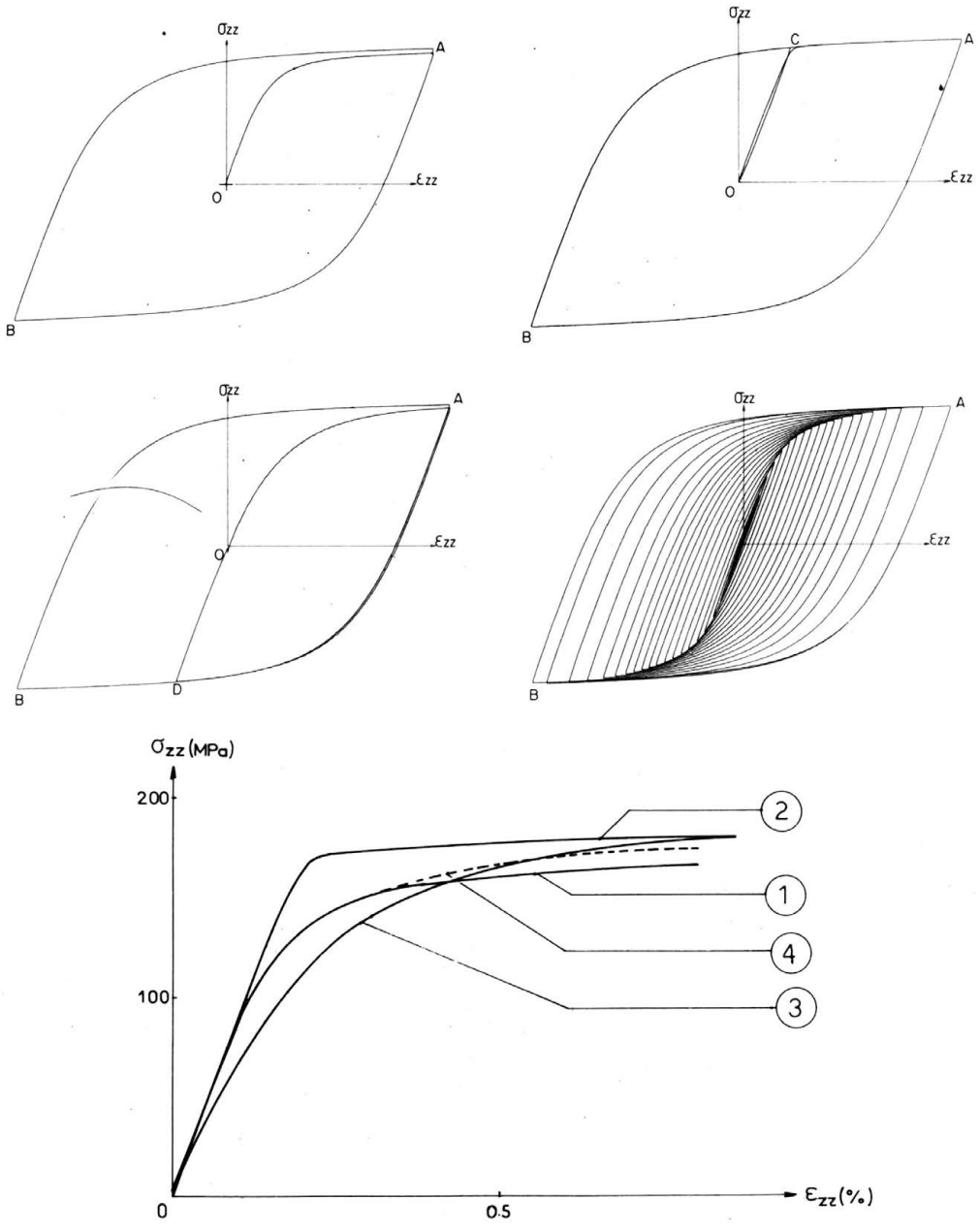

FIG. 8. Loading branches passing through the origin. Cyclic tension-compression. Cold drawn copper (test 507).

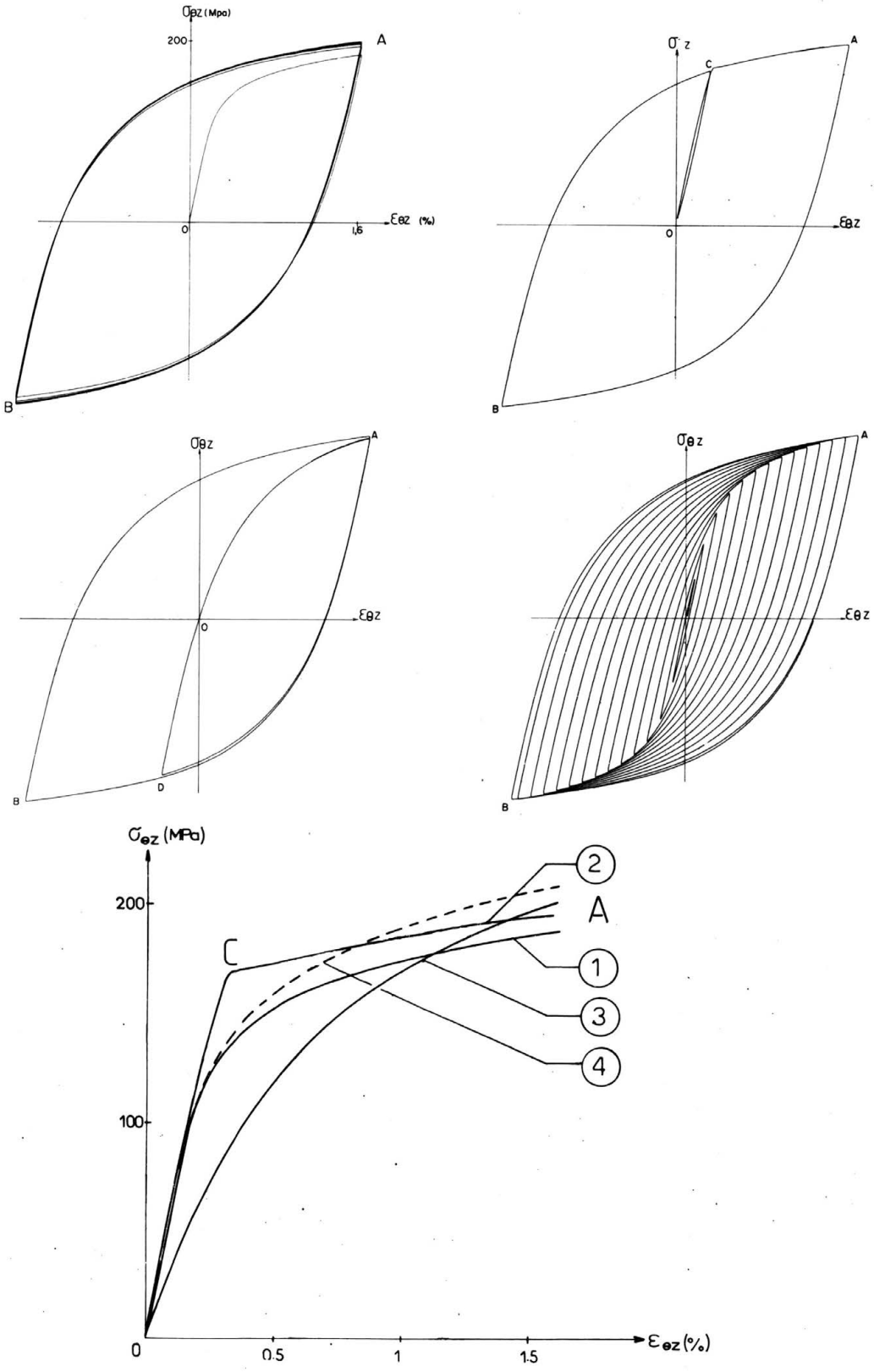

FIG. 9. Loading branches passing through the origin. Cyclic torsion. Commercial brass (test 603).

is about 10% of the stress value and may be explained by the fact that for this material macroscopic hardening is almost entirely erasable by the fundamental cyclic test [13]. This is not the case for the other materials, for which the erasable character is only partial and the difference between curves (*4*) and (*1*) is less than 5% of the stress value. The tangent at the origin of curves (*1*) and (*2*) is the same; it corresponds to the modulus value of the quasi-elastic behaviour, which is locally restored after any inversion. On the contrary, curve (*3*) possesses a tangent of lower value at the origin, since the path DO separates the origin from the preceding inversion D. Furthermore, curve (*2*) shows a rapid change of the tangent around point C where it reaches the branch BA. This change occurs in a relatively small area, about $1/100 \times 1/100$ of the large cycle dimension; by assimilating this small area to a point, the evolution of the tangent may be considered as discontinuous; it is due to the jump of the reference state from 0 (for the arc OC) to B (for the arc CA) (see Sec. A.3).

2.4. Evolution of the tangential modulus

Another way to verify some properties of the pure hysteresis contribution of the material behaviour is the analysis of the shape of the loading branches. This is done by determining the slope evolution along each loading branch. For that purpose the experimental results are expressed, in the loading branches space, in terms of coordinates $\Delta\varepsilon$ $(= \varepsilon - {}_R\varepsilon)$, $\Delta\sigma$ $(= \sigma - {}_R\sigma)$ (see Sec. A.3.d). The slope is defined by a tangent modulus M_x; for the simple push-pull test and for the cyclic torsion test we have respectively:

$$M_E = \frac{d\sigma_{ZZ}}{d\varepsilon_{ZZ}} \quad \text{and} \quad M_\mu = \frac{1}{2}\frac{d\sigma_{\theta Z}}{d\varepsilon_{\theta Z}}.$$

These moduli are determined by a spline technique and their evolutions are displayed versus $\Delta\varepsilon$.

A typical result is given by a cyclic torsion test with duralumin (Fig. 10). The modulus M_μ is determined only for the small cycles of strain amplitude $\pm 0.8\%$. As made conspicuous by the enlargement in the $\Delta\varepsilon$ interval [0,0.6%], the modulus evolution is identical for each branch, with the same value at the origin; this value is the modulus of the tangential elasticity behaviour which is locally restored after each inversion, i.e. the Young modulus E for push-pull tests and the shear modulus μ for cyclic torsion tests. At the beginning of each branch, the modulus evolution is parabolic-like with a horizontal tangent at the origin. This latter property corresponds to the existence of an inflexion point at the origin of the stress-strain first loading curve and, consequently, to the symmetry of this curve around the origin. Other results obtained previously with a stainless steel and a superalloy indicate the same properties [16, 17].

Furthermore, due to the large strain amplitude of the test, it appears obvious that the plasticity plateau is not horizontal: for large strains the tangential modulus tends to a finite value, of about 1/100 of the initial value. As this small slope is independent of the strain amplitude and of the cyclic hardening effect, it has to be considered as characterizing the pure hysteresis contribution; this rigidity is denoted $\hat{E}$ for a simple tension-compression test and $\hat{\mu}$ for a simple cyclic torsion test. Similar results were obtained with the other materials tested, for tension-compression as well as for cyclic torsion; the characteristic values of all the materials are given in Table 1 [18].

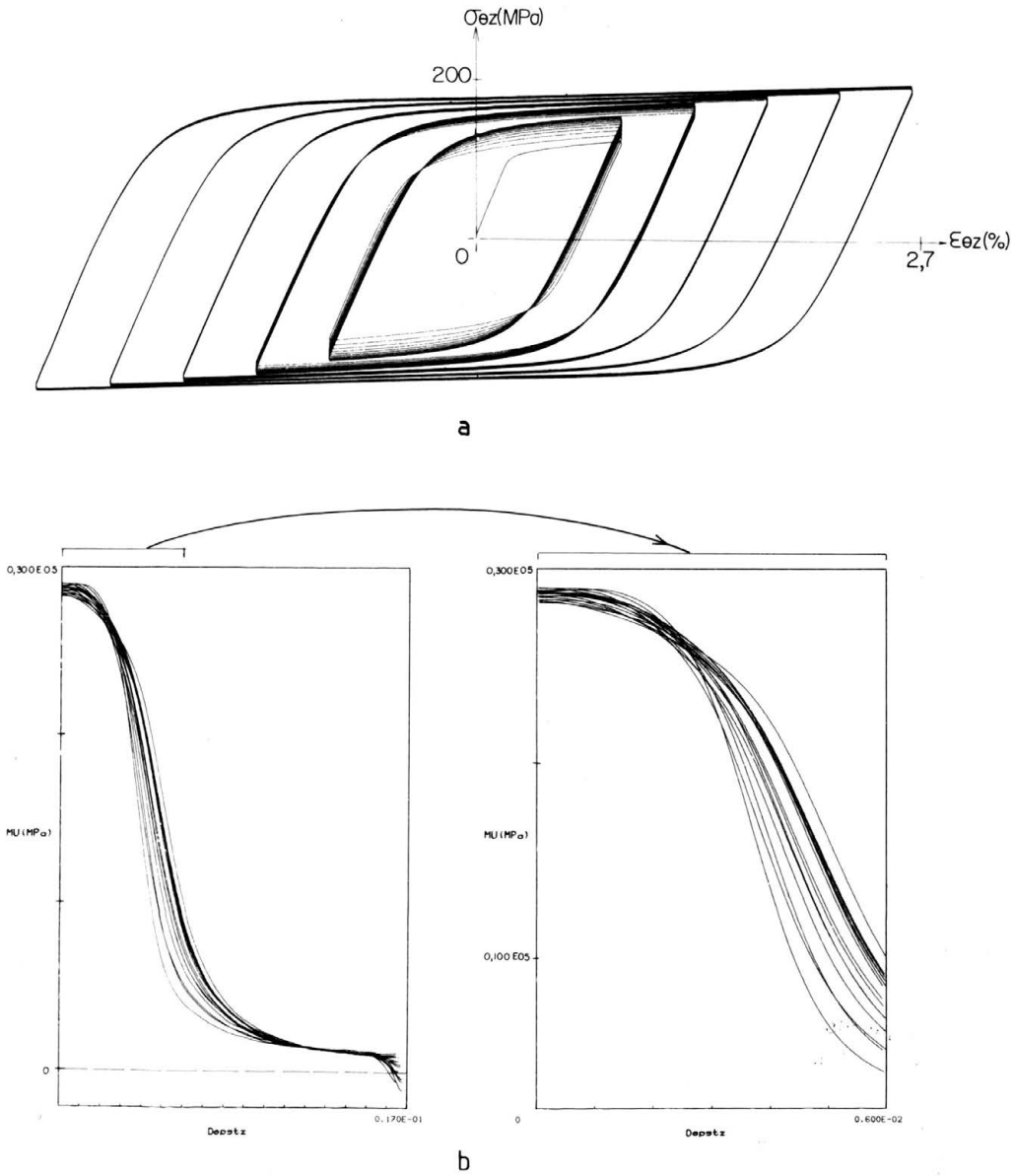

FIG. 10. Cyclic torsion test with increasing amplitude steps (a).
Slope evolution of the first step branches (b). Duralumin (test 703).

To be able to make comparisons, first between simple tension-compression and simple cyclic torsion tests for a given material and, secondly, between the different materials, the results are expressed in non-dimensional units: the tangential moduli and the strain difference are transformed into non-dimensional values, dividing by the initial value of the moduli (E or μ) and by the characteristic strain (ε^*_{zz} or $\varepsilon^*_{\theta z}$), respectively; we recall the definition:

$$\varepsilon^*_{zz} = \frac{Y_0}{E} \quad \text{and} \quad \varepsilon^*_{\theta z} = \frac{S_0}{2\mu},$$

Table 1. Essential characteristic values of different materials.

Materials		st. steel	eng. steel	c. dr. Cu	an. Cu	brass	dural.
E	GPa	199	197	95.6	102	82.9	71.9
$\pm\Delta E$		2	5	0.6	1.3	0.4	1.0
μ	GPa	77.6	78.8	38.3	41.2	33.2	28.7
$\pm\Delta\mu$		1.1	—	0.7	0.7	0.3	0.1
ν		0.280	0.254	0.289	0.291	0.262	0.197
$\pm\Delta\nu$		0.015	0.006	0.015	0.033	0.045	0.053
$\mu^*(E,\nu)$	GPa	77.7	78.5	37.1	39.5	32.8	30.0
$\pm\Delta\mu^*$		1.7	2.4	0.7	1.5	1.2	1.7
$\lvert\mu-\mu^*\rvert$	GPa	0.1	0.3	1.2	1.7	0.4	1.3
$\widehat{E}$	GPa	—	7.43	0.54	0.59	1.77	1.00
$\pm\Delta\widehat{E}$		—	0.73	0.08	0.05	0.13	0.20
$\widehat{\mu}$	GPa	0.39	1.71	0.18	0.087	0.27	0.26
$\pm\Delta\widehat{\mu}$		0.06	0.07	0.01	0.013	0.02	0.03
$\widehat{E}/E$	%	—	3.77	0.56	0.58	2.14	1.39
$\widehat{\mu}/\mu$	%	0.50	(2.17)	(0.47)	0.21	0.81	0.91
Y_0	MPa	300	614	208	62	245	322
$\pm\Delta Y_0$		9	24	3	8	10	17
S_0	MPa	170	370	130	36	143	127
$\pm\Delta S_0$		6	10	2	4	22	10
Y_0/S_0 ($\sqrt{3}=1.73$)		1.76	1.66	1.60	1.72	1.71	2.54
ε^*_{zz}	%	0.15	0.31	0.22	0.061	0.30	0.45
$\varepsilon^*_{\theta z}$	%	0.11	0.23	0.17	0.044	0.22	0.22

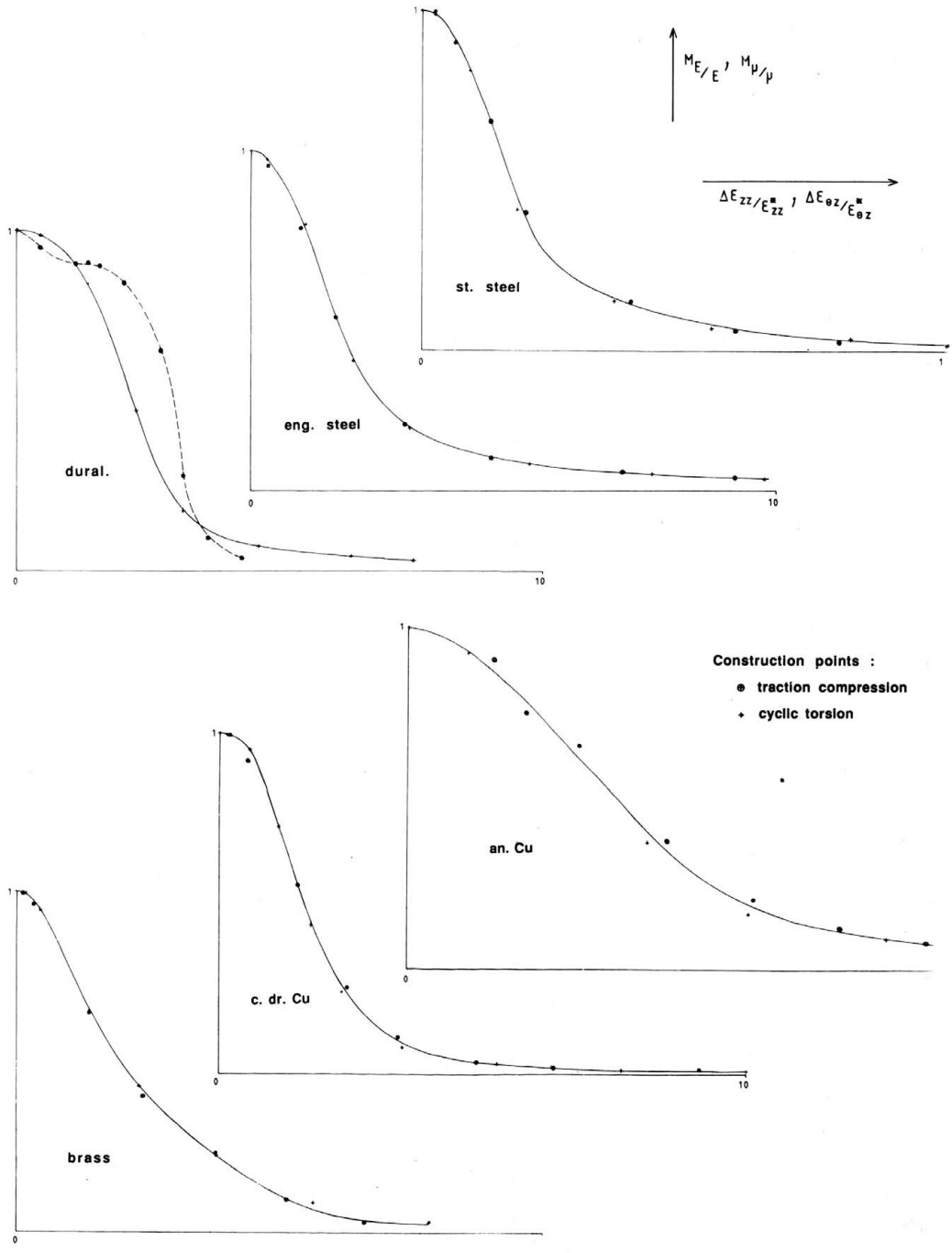

FIG. 11. Comparison of the slope evolution in cyclic tension-compression and torsion.

where Y_0 and S_0 are the stress limits in simple tension and simple torsion, respectively. In these non-dimensional axes and for a given material, the evolution of the tangential moduli appears to be independent of the test type (Fig. 11); the only exception concerns the duralumin for which the M_E evolution is particular and may be explained by a noticeable influence of cold drawing for this material. The points of Fig. 11 are only construction points obtained from experimental results (Fig. 10); they display the scattering between the two types of tests. The comparison of the mean curves characterizing each material is made in Fig. 12. For cold drawn copper, stainless steel and engineering steel the curves are almost identical. Annealed copper shows the slowest evolution. We verify, according to the definition of ε^*, that the inflexion point of the M_x evolution occurs for $\varepsilon \cong 2\varepsilon^*$, with the exception of annealed copper.

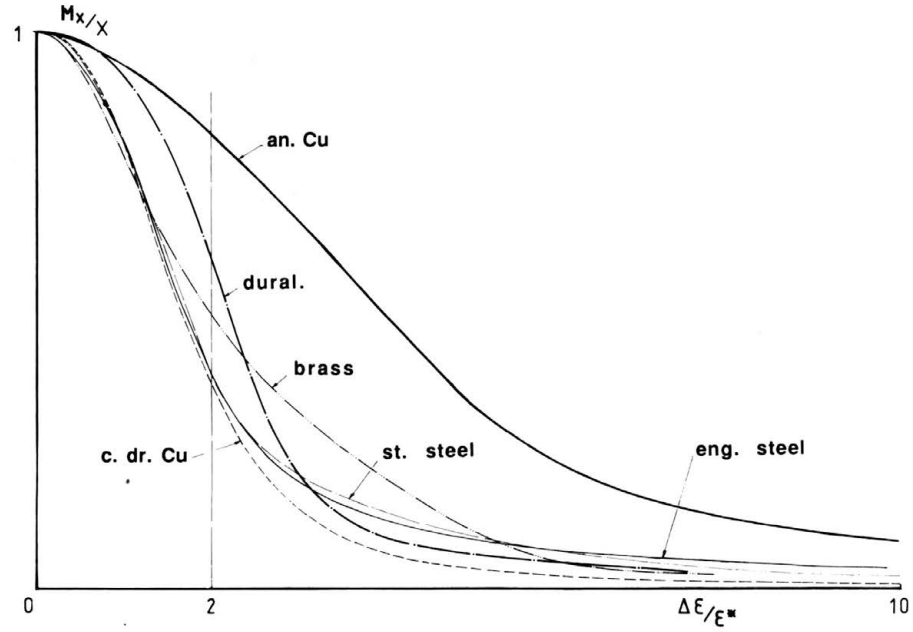

FIG. 12. Slope evolution: comparison of the mean curves characterizing the different materials.

3. Experimental microscopic support

The fact that the same properties are easily and fully recognized in a large variety of metallic materials is obviously related to a common explanation at a microstructural scale. This explanation, based on dislocation mechanisms, will be schematically illustrated by some of them, which are classical examples. As we are concerned here with a pure hysteresis behaviour, the pertinent mechanisms are those occurring on stationary cycles, after the stabilization of the microstructural phenomena.

A simple case of elementary mechanism is a single dislocation moving between two parallel walls on which it leaves pinned segments: this mechanism is analogous to a spring and a friction slider in series (Fig. 13). Under small stresses the dislocation will

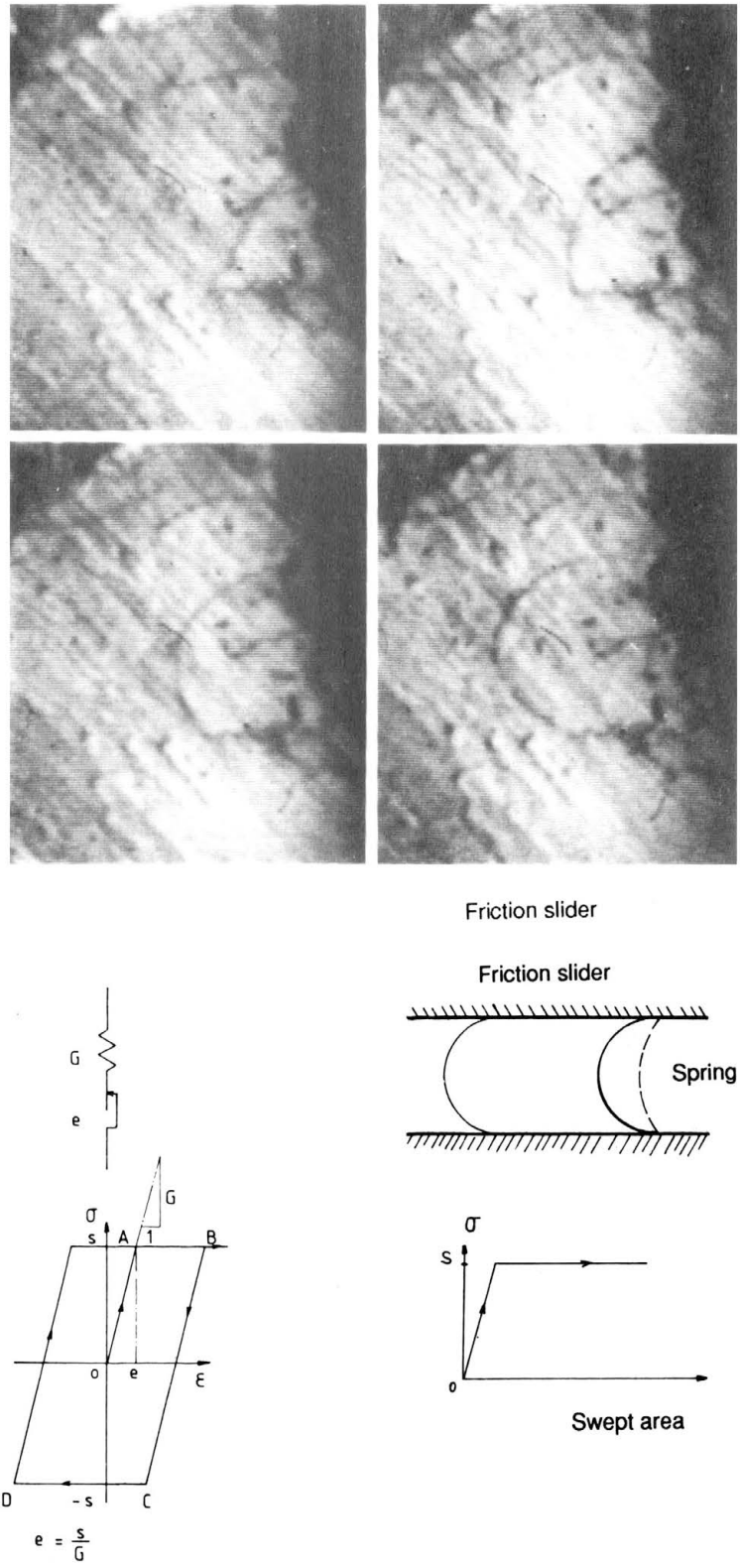

FIG. 13. Elementary microstructural mechanism equivalent to a spring and friction slider couple.

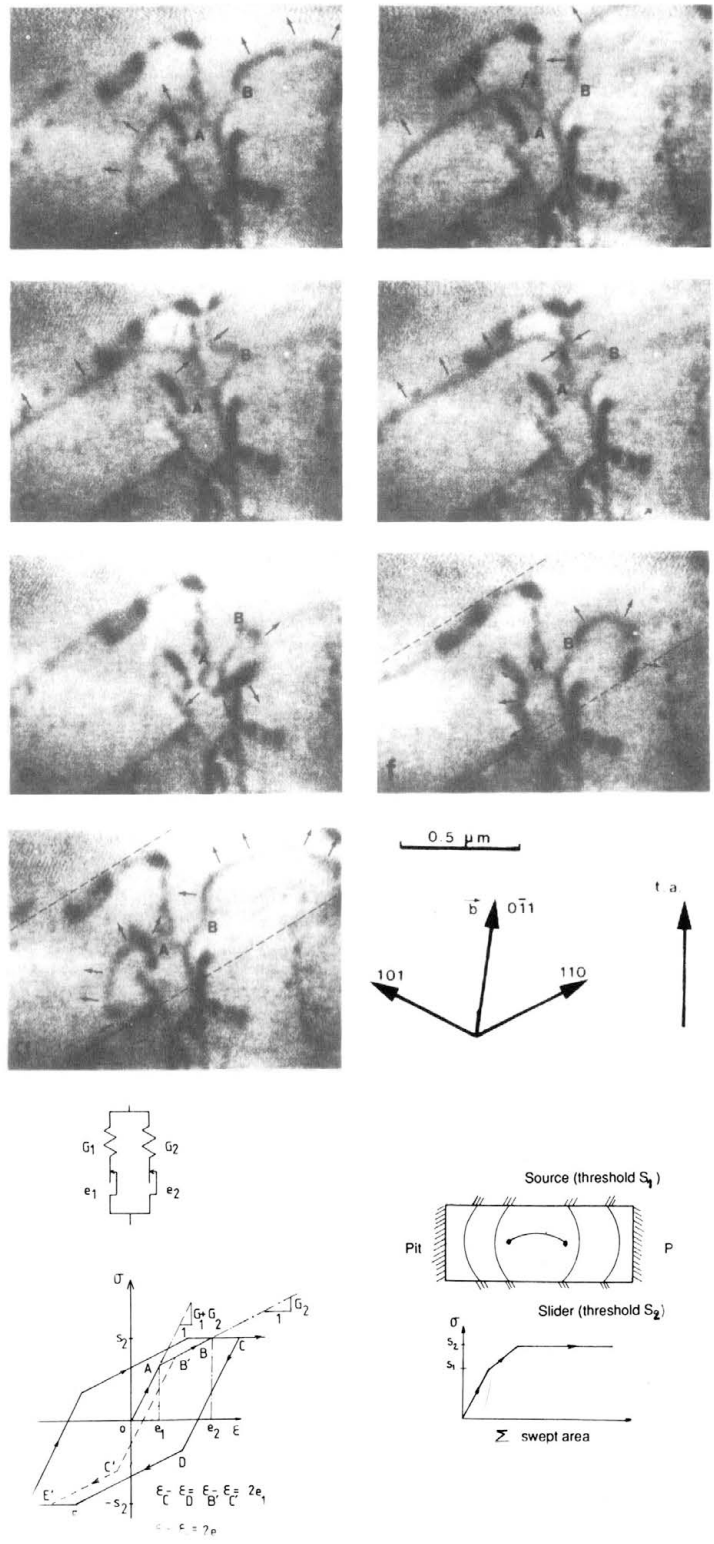

FIG. 14. Frank–Read source equivalent to two couples of spring and friction slider.

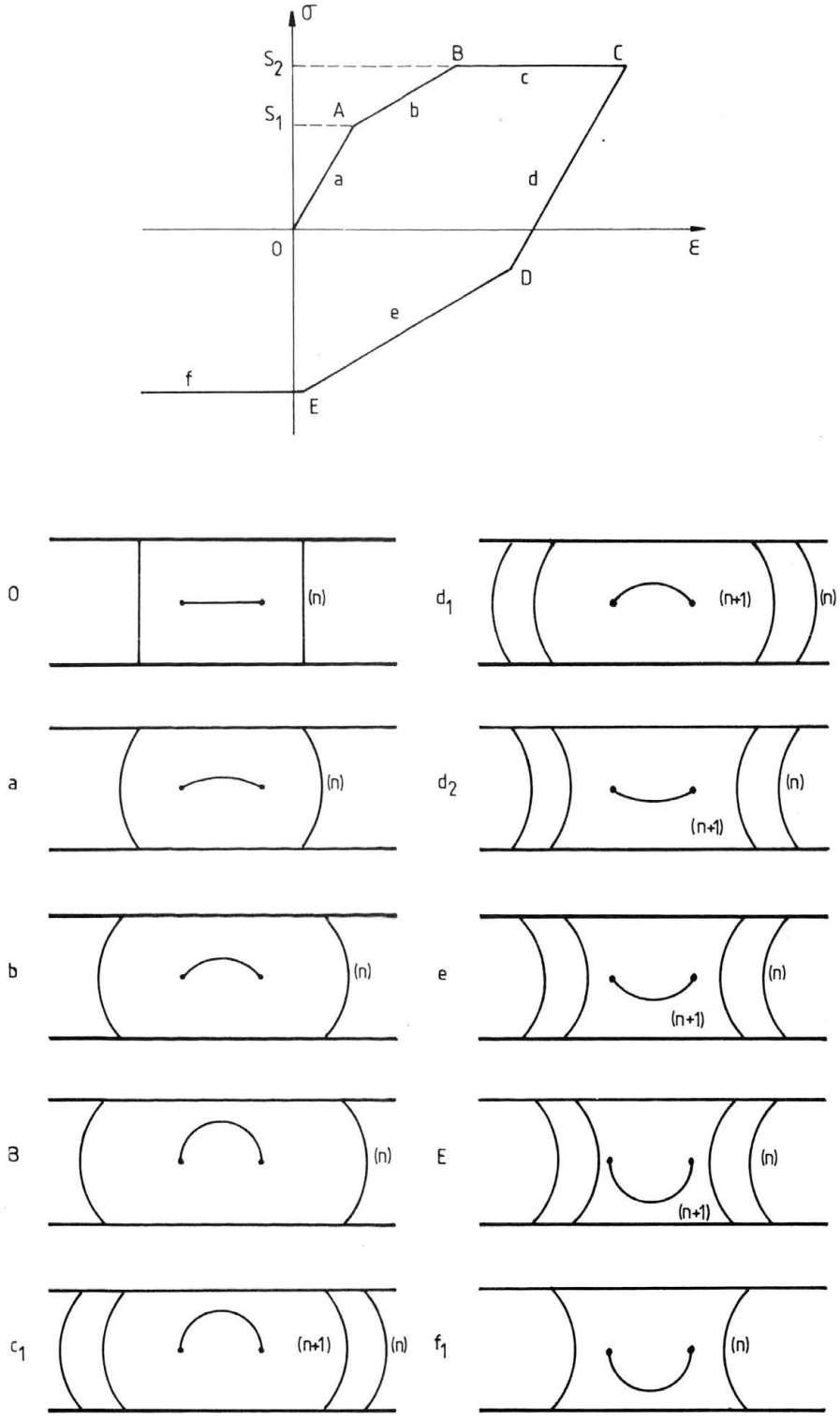

FIG. 15. Detail of the mechanism with a Frank–Read source operating between walls.

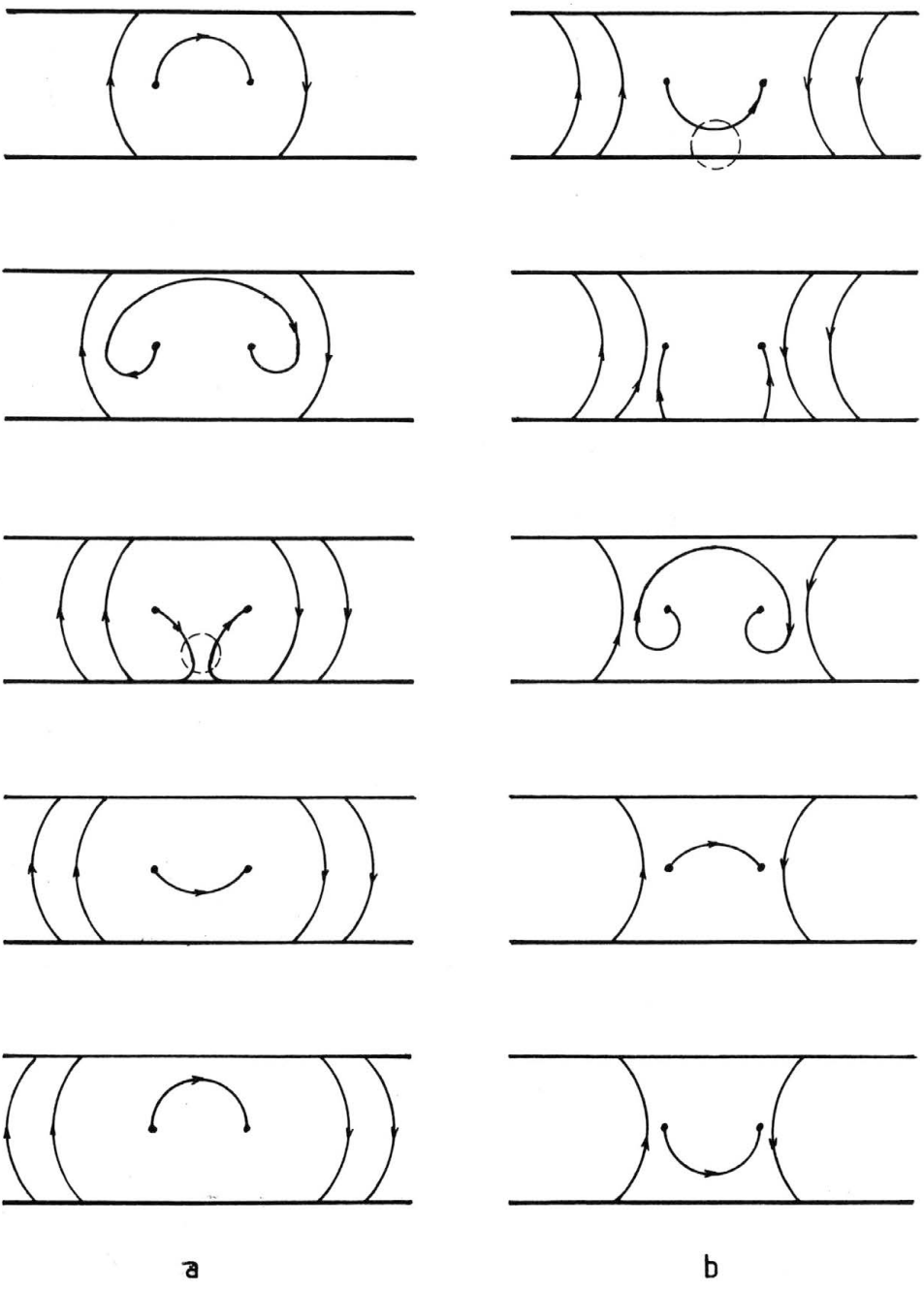

FIG. 16. Scheme of a loop emission (a) and absorption (b).

bend reversibly and behaves like a spring (line tension). Above a threshold stress **S**, the dislocation contact points on the walls will move and drag two segments along the walls: the behaviour is analogous to that of the friction slider (quasi-continuous pinning of the dragged segment in the walls). The diagram of stress versus area swept by the dislocation is of discontinuous elastic-plastic type. When the stress decreases, it is necessary for it to reach the opposite value $-\mathbf{S}$ before the contact points move in the reverse direction. In this first approximation, the behaviour thus appears really of pure hysteresis type. A slightly more complex case is that of a Frank–Read source operating between two parallel walls and characterized by two thresholds: S_1 for which the contact points on the wall move and S_2 (with $S_2 > S_1$ for example) for which the source emits a loop. This case is equivalent to a model with two spring-slider couples (Figs. 14 and 15).

A loop emission by a Frank–Read source is a bistable phenomenon, occurring on the plateau BC; for example two stable positions are state B and state c_1. The decomposition of the movement between two stable positions has already been observed and its classical scheme is recalled (Fig. 16a) (see for example [19]). The reverse movement of a source has also been observed, for instance recently in a superalloy between the cuboidal precipitates [20] (Fig. 16b). This bistable character means that the representative point of this mechanism moves by fits and starts on the plateau BC (Fig. 15). An estimation of order of magnitude indicates that, for usual dislocation densities, a loop emission corresponds locally to a deformation of about 10^{-4}. Thus if the accuracy of the strain measurement is better than this value, the fits and starts would be observable for a single source; but in real materials the combination of a group of sources operating randomly renders the starts and fits invisible even at an accuracy of 10^{-6}.

4. The assembly of microscopic elements to account for macroscopic behaviour

The elementary mechanisms operate at a microscopic scale (typically about 10^{-9} mm^3) and then a very large number of them are activated in a macroscopic sample. The activation thresholds of these mechanisms are scattered over a large spectrum, according to a few parameters: first the type of elementary microstructural mechanism whose two examples were examined previously, secondly the characteristic size of these mechanisms and thirdly the orientation of its glide plane with regard to the external loading (Schmid's factor); the compatibility conditions between adjacent grains or subgrains may also contribute to the spectrum amplitude [21]. The essential point consists in considering that the deformation of a real material is the *addition* and the *interaction* of a multitude of such elementary mechanisms which are characterized by a constant threshold, this threshold being continuously distributed between zero and a very large value.

This approach is an alternative to the classical one which considers a single, but global, elasto-plastic mechanism whose threshold varies with the applied conditions (strain amplitude, cycle numbers,...). The classical approach is equivalent to considering an "average" macroscopic mechanism, which can be meaningful when a single type of elementary mechanism controls the deformation. In contrast, the present approach takes into account the dispersion of the characteristics of microscopic mechanisms, and is more suitable when numerous different ones participate in the global behaviour.

The question now arises as to how to combine these mechanisms to account for the macroscopic behaviour. In the classical approach, the rules for combining different types of mechanisms and determining the "macroscopic yield stress" for instance depend on

their relative strengths and densities [22]. In spite of their efficiency, they can sometimes lack some fundamental basis, since a combination of different mechanisms, each having its own threshold, is supposed to give a macroscopic behaviour exhibiting a single threshold.

In the present approach, the problem is set in a different way, since we suppose that there is a priori no definite macroscopic threshold between an elastic and a plastic domain. The elementary microstructural mechanisms, each of which is represented by a spring and a friction slider in series, can be assembled in parallel: this is the only simple way to keep a reasonable physical meaning for the macroscopic assembly([2]). But as it happens, this is the type of assembly which has been used for describing the hysteresis behaviour of solid materials [10].

Thus it appears that the symbolic model constitutes a link between the microscopic and the macroscopic scales [18]. Due to both the symbolic unidimensional character of the model on one hand and the phenomenological type of the macroscopic description on the other hand, the analogy between the elementary microstructural mechanisms and the macroscopic behaviour is of qualitative type. Finally the symbolic model has a strong heuristic character. This was well established at the macroscopic scale since it allows a tensorial generalization to describe the real three-dimensional behaviour of materials [10, 13]; at the microscopic scale, the heuristic character is also obvious as will be thoroughly developed in the next paragraph.

The search for a better understanding of solid material behaviour has been an open question for a long time. For instance, we should mention the work done by BOUASSE [24], at the beginning of this century, concerning cyclic torsion tests on wires; he explains his experimental results by introducing almost all the mechanical properties of the pure hysteresis behaviour, but without the help of the symbolic models. On the other hand, for thirty years a series of studies has made reference to the significant work done by MASING [25] which is, in our knowledge, the first to propose the assemblage of spring-friction slider couples for explaining the material behaviour. Some studies consider only a limited number of spring-friction slider couples, like the multi-layered model [26] or the wall-channel model [27], but in order to be able to describe real behaviours, some complementary ingredients had to be added. Holste and BURMEISTER [28], and POLAK and KLESNIL [29] considered, like PERSOZ [23], a continuous distribution of spring-friction slider couples; but the essential role played by inversion states, and then by the discrete memory, was not evidenced. In a recent book CHRIST [30] put in use the rheological model with springs and friction sliders in view of studying the cyclic hardening behaviour under complex loadings. But as in the case in some preceding studies, the author does not introduce the essential notions of reference state and discrete memory: the theoretical modelisation he proposes at the end of his book is a step by step evolution of a finite number of elements of individual given characteristics. This modelisation is similar to the one of Masing, the difference being that Christ, with the help of computers, takes into account thirty elements, while Masing has used only ten elements. In contrast, a complete interpretation, both mechanical and thermodynamical, of the continuously distributed model has been proposed by GUELIN [10], allowing to arrive at three-dimensional behaviour description [11 to 13]. One aim of this paper, among others, is to complete

([2]) Other types of assembly may be envisaged, but they do not possess the properties of simplicity and physical interpretation as the parallel assembly [23].

the latter study by adding, for the case of crystalline materials, a complementary interpretation with elementary microstructural mechanisms responsible for the deformation of these materials.

For the sake of simplicity, the symbolic model is briefly recalled in the appendix, together with its main properties concerning irreversibility, local restoration of the behaviour, discrete memory and restorable neutral state. However, the way in which the model can help in the description and interpretation of local internal stresses or elastic and plastic strain is discussed in the next paragraph, using some tools defined in the appendix. Finally, the relative importance of viscosity, and subsequently the validity domain of the pure hysteresis behaviour, will be thoroughly discussed.

5. Discussion on micro-macro correspondence

5.1. Local internal stress

The topological diagram (see A.2) allows us to complete the analogy between the macroscopic behaviour and the microstructural phenomena, particularly by displaying the notion of local internal stress. Indeed for each element of the model, the spring and the friction slider support the same stress: this is the local internal stress σ_i of the corresponding microstructural mechanism. Since we have:

$$\varepsilon_r = \frac{\sigma}{g(e)} \quad \text{and} \quad e = \frac{s}{g(e)}$$

we see that the representative line of the topological diagram gives an image of the local internal stress distribution, within the multiplying factor $1/g(e)$.

It then appears obvious that when the macroscopic stress is zero, the internal stresses may not be zero in general, but have only a mean zero value (Fig. 26). It is only for the initial neutral state that the local internal stresses are zero for each element. The fundamental cyclic test enables us to restore this initial neutral state by progressively making uniform the local stress of each element to a value tending to zero (Fig. 27).

Even for an annealed material there may locally exist initial internal stresses σ_{i0} originated by cooling or incompatibilities between grains [21] for instance: this situation may bring a mechanism near the threshold and a small stress increase may then activate this mechanism. But since the material behaves globally as an annealed material, we may suppose that to each mechanism A, in an initial unsymmetrical situation, corresponds its opposite mechanism B (Fig. 17a,b). The behaviour of these two mechanisms is equivalent to the addition of two symmetrical mechanisms A_e and B_e, one of small threshold $S_m = S - \sigma_{i0}$ and the other one of large threshold $S_M = S + \sigma_{i0}$ (Fig. 17c). The correspondence between these four mechanisms becomes obvious in the topological diagram, by using the stresses as variables (Fig. 17d).

This situation can be observed for instance during in situ cyclic deformation of an A1-0,7 wt% Li alloy (Fig. 18). Before the inversion, a dislocation emitted from a dense wall moves in its glide plane: it is mechanism A (steps 1 and 2 Fig. 18); after the inversion this mechanism stops and another dislocation becomes activated in another glide plane: it is the mechanism B (steps 3 and 4 Fig. 18). We are in presence of two asymmetrical mechanisms alternatively activated.

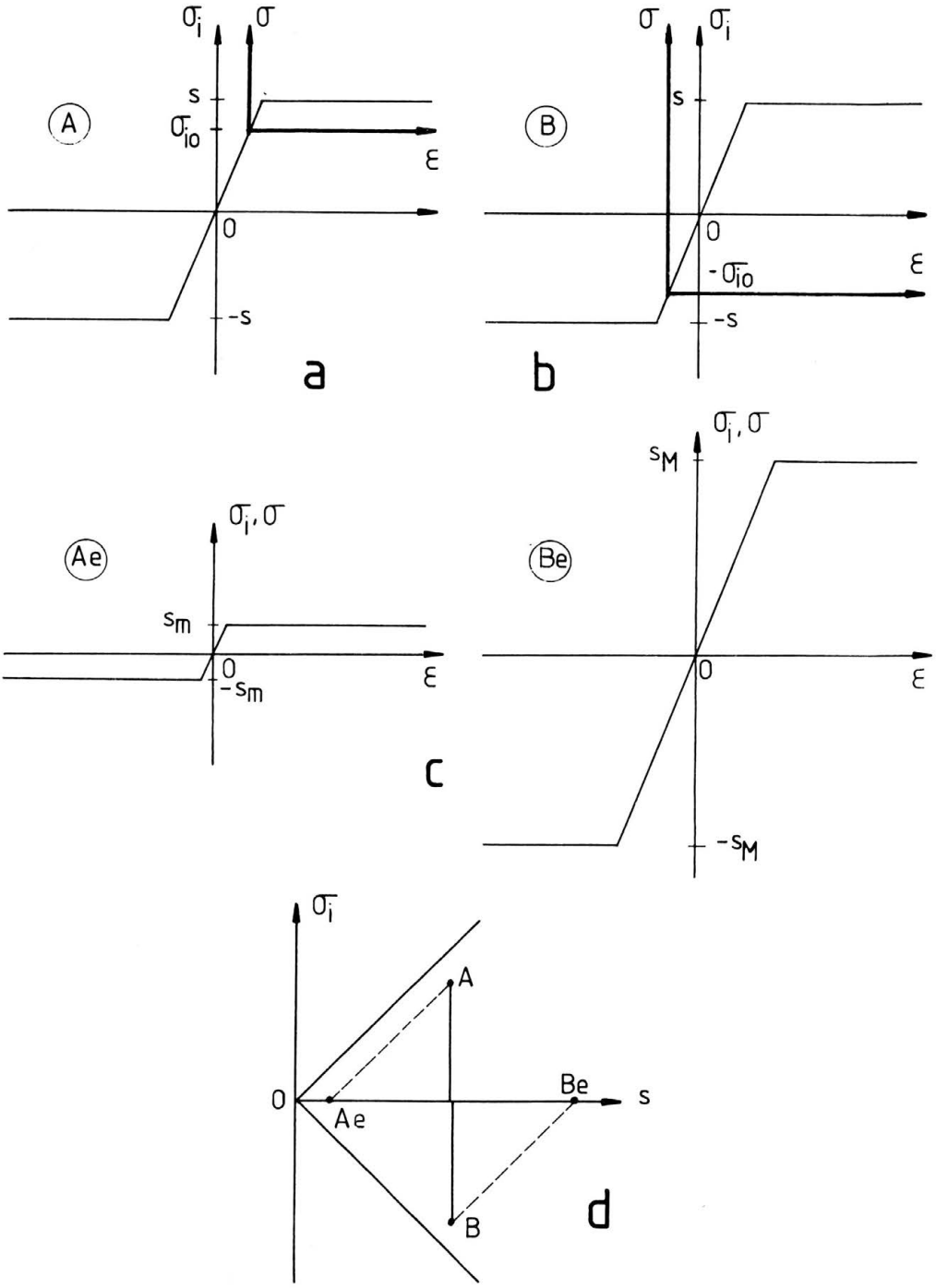

FIG. 17. Equivalent mechanisms to take into account the incompatibility between grains: (a) an elementary mechanism influenced by grain incompatibility; (b) its opposite mechanism; (c) the two equivalent mechanisms; (d) the position of the four mechanisms in the topological diagram.

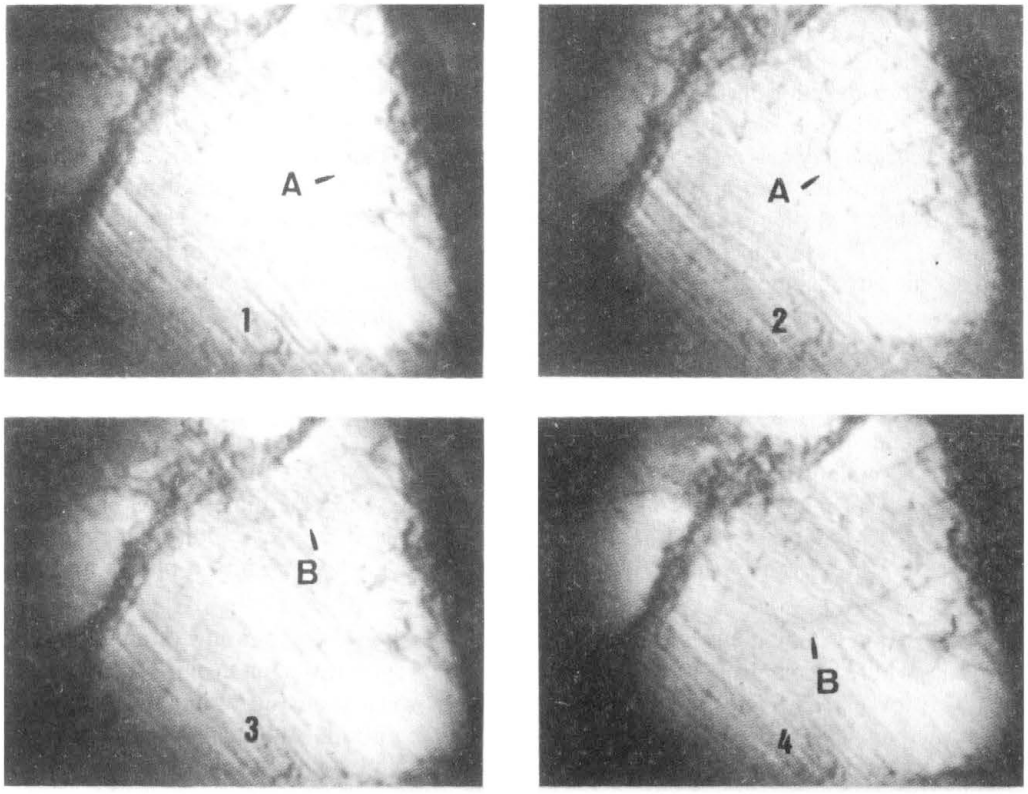

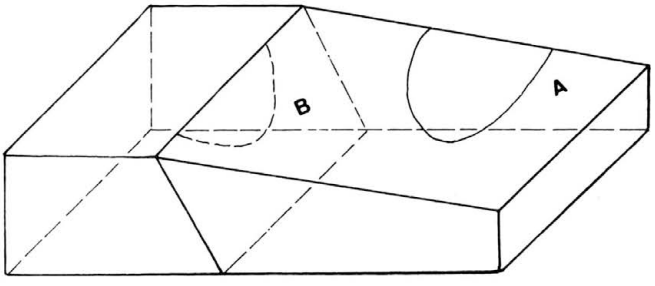

FIG. 18. Example of the mutual grain influence.

5.2. Elastic, plastic and total strains

The symbolic model with its microstructural interpretation allows a better understanding of the role and the importance of the notions of plastic strain and total strain in the description of the real material behaviour. For an individual elementary microstructural mechanism, equivalent to a spring-slider couple, the plastic strain ε^P has an obvious physical meaning: it is the friction slider deformation, which is directly related to the dissipated energy. Thus the plastic deformation ε^P may be considered as a true physical variable in the behaviour description of this individual mechanism.

But the situation is quite different for a distribution of microstructural mechanisms (case of real polycrystals): then there exists a continuous distribution of individual plastic strains ε_i^P, between zero and the applied macroscopic strain ε. The global macroscopic plastic strain ε^P is then a mean value depending on the distribution of thresholds S_i and rigidities G_i. Thus it appears that the macroscopic parameter ε^P does not have a simple microscopic physical meaning, and consequently its determination, if considered necessary, becomes a matter of convention. Nevertheless some specific cases exist where we may consider that the macroscopic behaviour is the addition of N identical microstructural mechanisms; in this case the plastic deformation keeps a physical meaning for the whole. An example is that of a single crystal in single slip conditions, with a single obstacle of well defined threshold, or a large-grained polycrystal hardened with regularly spaced precipitates of similar strength.

The study of material deformation is foreseen in view to determine behaviour equations useful to engineers. And at the macroscopic scale there exist additional reasons, of decreasing importance, that may incite us not to split the strain into a plastic and an elastic contribution:

- The strain is an extensive thermodynamical variable; we do not know of any domain of physics where an extensive variable is split into different terms in an evolution equation.
- The total strain is a direct observable quantity which is measured independently of the behaviour assumptions; this is not the case for the plastic strain (although a simple macroscopic definition can be given in the case of simple loadings).
- In the case of finite and/or complex strain, like a combination of tension and torsion, the definition of a plastic strain tensor gives rise to theoretical problems not yet resolved.
- It is not easy to realize a cyclic test at constant plastic strain rate (what happens at the origin and after the inversions?).

For all these reasons it appears more accurate to avoid the use of a plastic strain, at the macroscopic scale, and to express the behaviour through the total strain.

Furthermore the strain irreversibility explains the existence of a fatigue limit for small strain amplitude tests: however small the cyclic amplitude might be, the cycle area has a non-zero value indicating the existence of energy dissipation. Thus, as the distinction between elastic and plastic strains appears somewhat artificial, so does the distinction between high and low cycle fatigue. Since damage is an increasing function of irreversibility, i.e. of cycle area, it is expected to be significantly lower at low strain amplitude, but however not zero.

5.3. Elastic and plastic behaviour

Due to the threshold distribution of the elementary microstructural mechanisms, the ideal elastic or plastic behaviour which exists locally, vanishes in the global macroscopic

behaviour. They only appear in very particular conditions and therefore we use the terms of quasi-elastic behaviour and quasi-plastic behaviour at the macroscopic scale. In fact, at the origin and just after any inversion state, all the elementary microstructural mechanisms behave instantly like an elastic body; but due to the fact that the distribution of the mechanism thresholds begins at zero, the *elastic behaviour* at the macroscopic scale is *tangent* to the real behaviour.

Likewise *plastic behaviour*, at the macroscopic scale, is an *asymptotic* one: when the strain increases, more elementary microstructural mechanisms become activated and behave plastically, and for large strains the increase rate of active mechanisms declines and tends to zero. So the real material may approach, more and more closely, a pure plastic state but theoretically never really reach it, although a great number of elementary microstructural mechanisms behave strictly as plastic. The ideal situation shown by the pure hysteresis model gives a zero slope asymptote, since the total load supported by the model is finite (see A.1). For this reason one can speak of a *plastic limit* (Y_0 for simple tension, S_0 for simple torsion) and not of a plastic criterion (or threshold); this latter term has a meaning only at the microscopic scale for a given elementary mechanism.

For real materials the situation is less simple. Let us first consider the case of a cyclic loading at a given strain amplitude. A pure hysteresis is reached after stabilization of the stress-strain cycle, i.e. after hardening saturation for the considered strain amplitude. We observe experimentally for most materials, like duralumin (Fig. 10), that the slope of the asymptotic plastic behaviour is not exactly zero and appears constant and independent of the strain amplitude, for the order of magnitude of a few percent. This property may be interpreted as a *residual rigidity* which may be ascribed to both some kinematic hardening due to dislocation accumulation, and the contribution of a few microstructural mechanisms which continue to behave elastically even for large strains. Experimental results indicate that this residual rigidity ($\widehat{E}$ for tension or $\widehat{\mu}$ for simple torsion) is of the order of a few percent of the initial rigidity (E or μ). A schematic representation of this property is obtained in the unidimensional case by a single spring in the symbolic model (see A.1); in the real three-dimensional case the solution is given by the addition of a reversible contribution to the irreversible one [15]. In the classical elastic-plastic theory the residual slope is denoted as a hardening slope. If we now consider a monotonic loading, the stress-strain slope in the quasi-plastic region reveals a supplementary effect due to hardening and consequently an apparent rigidity greater than the residual rigidity. Finally hardening (or softening) is characterized by the evolution of the limit stress Y_0 or S_0; in the unidimensional case it may be simply described as a modification of the distribution of the model rigidities: the function $g(e)$ evolves but keeps its properties (Sec. A.1). Thus the behaviour is modelized as an *evolutive pure hysteresis behaviour* (we recall that in the general three-dimensional case this is obtained through a projection method, see for example [13]).

5.4. Discrete memory of particular events of the loading

The notion of discrete memory, displayed for example by a small cycle described inside a large cycle (Fig. 19), may also be easily explained at the microscopic scale. When the material state arrives at C, after the path BC, all the elementary mechanisms whose

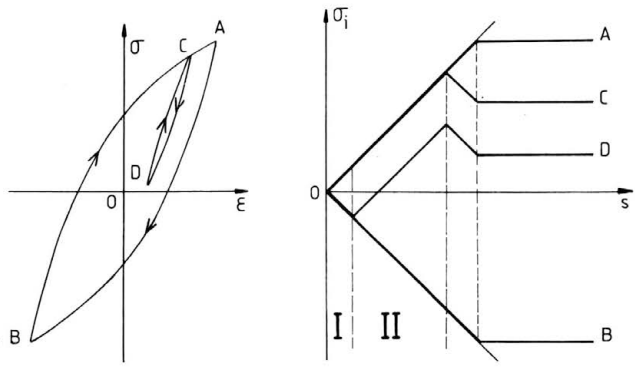

FIG. 19. Scheme of a small cycle described in a large cycle and its correspondence in the topological diagram.

threshold is smaller than $S_c = \frac{1}{2}(\sigma_C - \sigma_B)$ have been activated. After the inversion at C, these mechanisms stop operating. Along path CD the elementary mechanisms tend to operate in the reverse direction, beginning with those of small threshold; at D only the elementary mechanisms whose threshold is smaller than $\frac{1}{2}(\sigma_C - \sigma_D)$ are activated in the reverse direction; they are the mechanisms of group I (Fig. 19). Consider now the elementary mechanisms of group II, whose thresholds lie between $\frac{1}{2}(\sigma_C - \sigma_D)$ and $\frac{1}{2}(\sigma_C - \sigma_B)$. All of them were activated at state C, after the path BC. Along the path CDC, the internal stress of the mechanisms of group II has first decreased and then increased by the same amount, as the mechanisms are not activated (Fig. 19). By returning to state C, and for the macroscopic stress σ_C, all the mechanisms of group II are ready to be activated at the same time, since their internal stresses reach the threshold value at the same time. This gives rise to the discontinuity of the branch DCA at the crossing of state C. One sees that the memory of the preceding inversion states, which is of discrete type, has the material itself as a support: it is marked by angles in the distribution of the internal stresses of the microstructural mechanisms and these angles either stay constant during the loading or are entirely erased at the crossing of particular loading states. We recall that the discontinuity at C of the branch DCA is taken into account in the constitutive equation by the jump of the reference state from state D to state B. The detection of such a crossing in the general three-dimensional case is obtained using thermodynamical rules (see for example [13]).

The experimental verification of such a discontinuity is made by the curves of type 2 passing through the origin (see Sec. 2.2); an enlargement of these curves is given in Fig. 20. We see that within an accuracy of about 1% the curves at the crossing at C are discontinuous. Additionally it appears that the measurement accuracy is precise enough to show some effects of smaller order of magnitude: the discontinuity may occur with or without a bounce, depending on the material type. These results also show clearly the irreversible character of the strain; the unloading after the inversion at state C cannot be considered as elastic, since the small cycle CDC shows that its area is not zero. These results agree with those already obtained seventy years ago by DALBY [31] with different metallic materials.

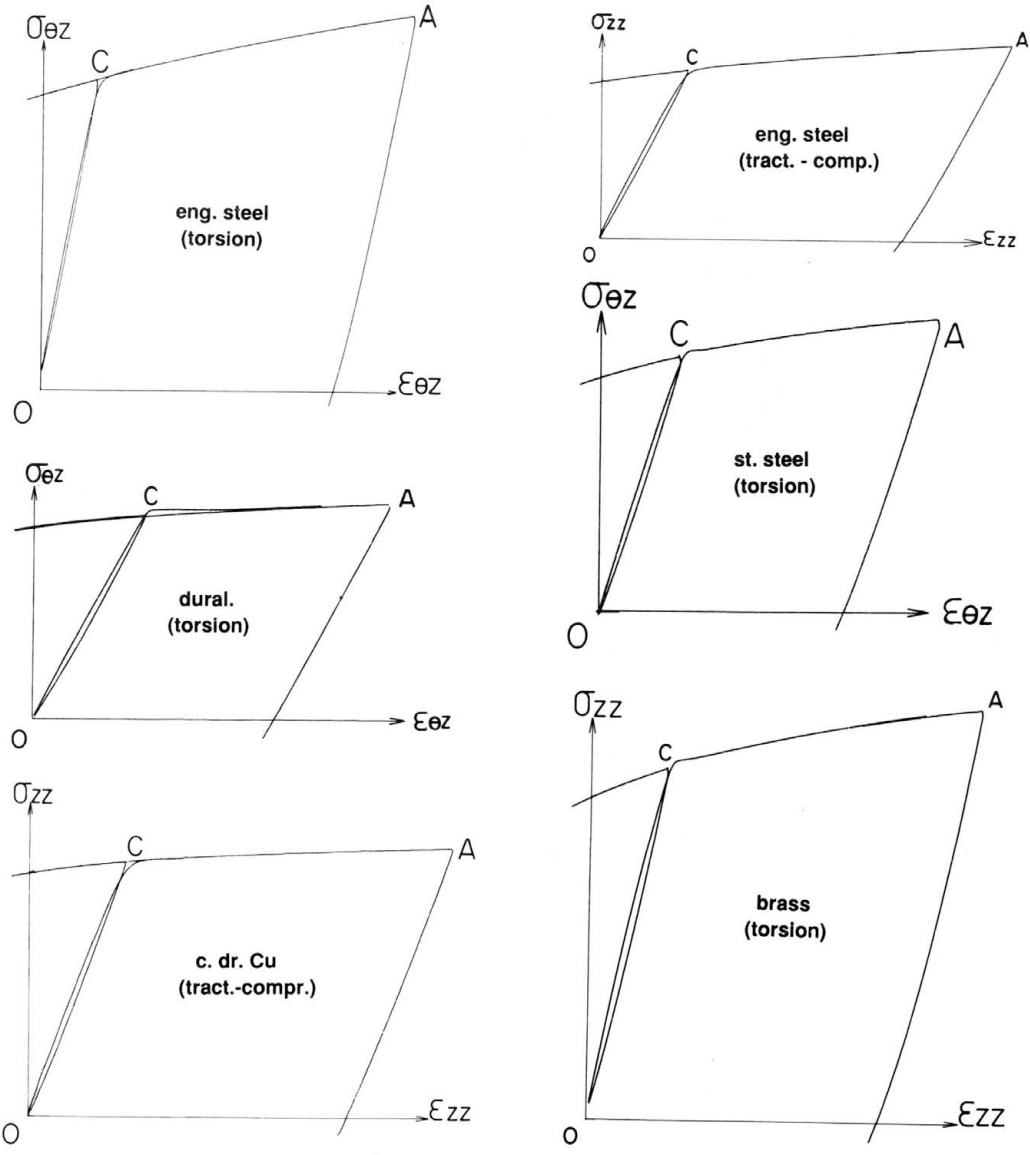

FIG. 20. Experimental results showing first the slope discontinuity produced by a small cycle described in a large cycle, and secondly the irreversibility of the strain (see Fig. 19).

6. The relative importance of viscosity and of pure hysteresis contributions

Let us consider a sample of material submitted to a symmetric cyclic test. The material is supposed to be in an annealed metallurgical state so as to be under the influence of no previous strain history. The test is strain-controlled at a constant low strain rate and at room temperature, i.e. a relatively low temperature; the strain amplitude $\pm\varepsilon_1$ is of the

order of magnitude of a few 10^{-3} and corresponds to the domain of low cycle fatigue (Fig. 21a).

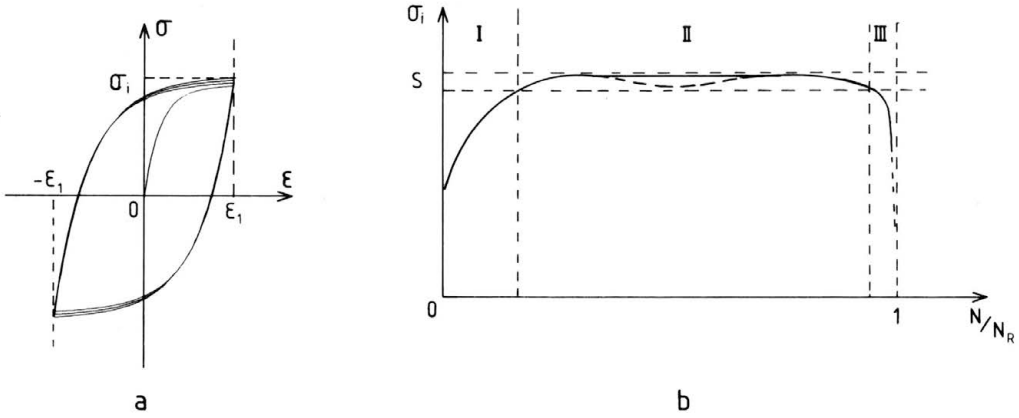

FIG. 21. Symmetric cyclic test.

In the stress-strain diagram the test will essentially exhibit a hysteresis loop, but its evolution during the cyclic test may evidence some other physical phenomena. In a first step this situation may be analyzed through the evolution of the stress value at the inversion points versus the number of cycles N (Fig. 21b), in which we observe the existence of three main stages: at the beginning the stress increases during a few dozens of cycles (stage I), then it stays almost constant during a great number of cycles (stage II) and at the end we see a rapid decrease (stage III). We notice that the repetition of the stable hysteresis loop is the most important stage, as it lasts generally during about 90 to 95% of the sample life, measured by the number of cycles up to rupture N_R. It then seems reasonable in this case to describe the material behaviour in stage II by a pure hysteresis phenomenon and to account for the particular behaviour of stages I and III through a combination of this basic hysteresis mechanism with additional processes evolving from hardening or damage. These additional mechanisms can be taken into account through an evolution of the plastic limit stress of the pure hysteresis behaviour.

However, even in stage II where the hysteresis behaviour is most obvious, one can wonder whether this behaviour is an "intrinsic static" one, i.e. depends only on the material structure, or if "kinetic" parameters such as temperature or strain rate, which control viscosity, can have a noticeable influence on the hysteresis characteristics.

The influence of viscosity may be evidenced, for instance, by relaxation tests. The amount of stress relaxation is well known to increase when the initial strain rate is increased, whereas the stress level reached after relaxation is independent of the initial strain rate (see for instance [32]). As an example of order of magnitude, the stress relaxation measured during 600 s after a test run at a strain rate of 10^{-4} s^{-1} is less than 10% for a stainless steel at room temperature.

Among the mechanisms responsible for irreversible deformation of crystalline materials in usual test conditions, two main classes are ordinarily defined, according to whether the overcoming of obstacles by dislocations is helped by thermal vibrations (thermally activated phenomena) or achieved only by the applied stress (athermal phenomena). The

first type of obstacles is that for which the overcoming process involves a coordinated motion of a small number of atoms, which can be achieved by a stress-assisted thermal fluctuation, with a "reasonable" probability of success. This is usually the case for obstacles of short range stresses (Peierls friction stresses, forest cutting,...). The second type of obstacles to dislocation motion is that which is associated with long range stresses, whose overcoming involves such a large number of atoms that the probability of the corresponding thermal fluctuation is negligible. This is usually the case of internal stresses. Of course, the frontier between these two types of overcoming processes is not sharp since probabilities are involved; furthermore the frontier definition depends on the time scale considered. Indeed if we consider longer and longer experiment durations, the ratio of the numbers of athermal to thermal activated processes will decrease and tend theoretically to zero at infinite times. In other words, if we consider infinite times, all the mechanisms responsible for irreversible deformation of crystalline materials have to be considered as only thermally activated phenomena. But for practical finite times scales (i.e. duration of a straining test, lifetime of a bridge,...) we will always have to deal practically with a separation between thermally activated phenomena and athermal phenomena. The latter account for the pure hysteresis behaviour and the term "viscosity" is the macroscopic equivalent of the influence of thermally activated phenomena on the global behaviour of materials, as measured through stress relaxation tests. In Fig. 22, relaxation curves (*1*), (*2*) and (*3*) correspond to different viscosities, or equivalently to thermally activated processes *with different characteristic times*. The specimen which shows the smallest proportion of viscous contribution is that which deforms at the lowest stress rate, i.e. specimen (*3*).

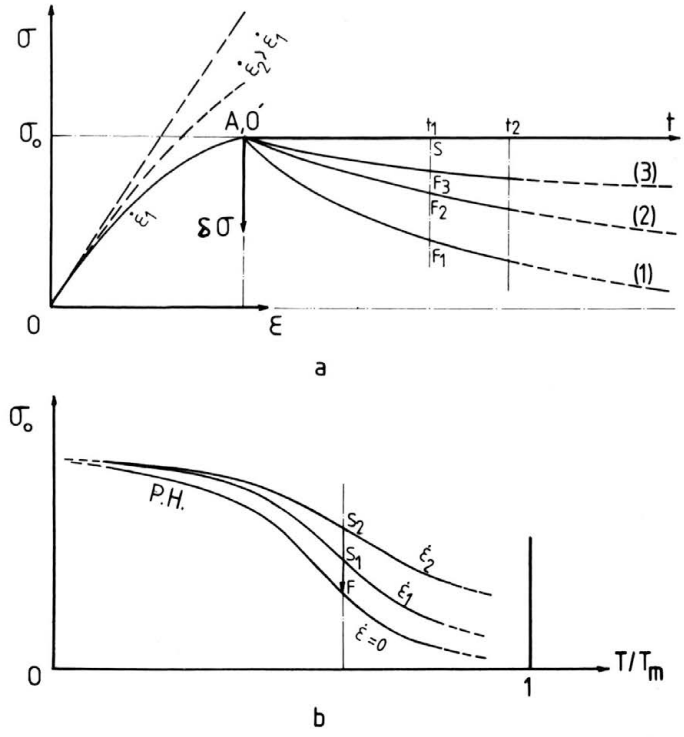

FIG. 22. Definition of the pure hysteresis and viscosity contributions.

Since we consider finite times, the end of the curves has to be considered for instance at t_1 (or t_2) and then the stress decrease SF_i due to relaxation increases with the initial relaxation stress rate.

Let us now consider a given material and the evolution of its initial stress σ_0 at different temperatures and strain rates. The stress σ_0 is a decreasing function of temperature at constant strain rate, or increases with strain rate at constant temperature. These evolutions may be schematically represented by Fig. 22b, where the curves $\sigma_0(T/T_m)$ are plotted at constant strain rate. By definition the amount of thermally activated processes decreases to zero at zero temperature and attains maximum at $T = T_m$, thus explaining that the curves are very close at $T = 0$ and spread out from one another at $T = T_m$. The bottom curve at $\overset{\circ}{\varepsilon} = 0$, corresponds to the pure hysteresis behaviour. For $\overset{\circ}{\varepsilon} \neq 0$ the stress interval $S_i F$ at constant T corresponds to the stress decrease by relaxation and consequently to the amount of viscous behaviour in the total behaviour. This situation shows that materials preferentially exhibit a hysteresis behaviour at low temperatures and surprisingly low strain rates, which are the experimental conditions which minimize viscous effects. These conclusions qualitatively agree with experimental observations [33]. This explains the precautions taken to render conspicuous and to study experimentally the pure hysteresis properties (see Sec. 2): the tests should be carried out at the lowest strain rate consistent with experiment duration (i.e. about 10^{-4} s^{-1}), and at relatively low temperature, although this last condition is usually fulfilled at room temperature for a number of materials. Furthermore, due to the smallness of the viscosity contribution, the constancy of the strain rate enables us to consider the behaviour as an equivalent pure hysteresis behaviour.

7. Concluding remarks

The experimental macroscopic results presented here show that it is possible, with a large variety of metallic materials, to identify all the properties of the pure hysteresis behaviour. Thus a justification is supplied, validating the corresponding discrete memory constitutive scheme used to describe macroscopic behaviours. Furthermore it is shown that the operation of a simple elementary microstructural mechanism, at the scale of dislocation motion and responsible for the material deformation, may be symbolically represented by a spring attached to a friction slider. And then the assemblage of a great number of elementary microstructural mechanisms may be exhibited by the same symbolic model of springs and friction sliders as the one which is at the foundation of the discrete memory constitutive scheme. Thus it appears that there exists a correspondence between the elementary mechanisms at the microscopic scale and the discrete memory constitutive scheme describing the macroscopic behaviour. This correspondence, or analogy, is evidently of qualitative type due to the phenomenological type of the macroscopic behaviour description considered here, and to the contrast between the unidimensional character of the symbolic model and the necessity of a three-dimensional description of the macroscopic behaviour. One of the main points is the fact that the behaviour of crystalline materials is considered as the result of the addition and the interaction of a multitude of elementary microstructural mechanisms which are characterized by almost constant thresholds, these thresholds being continuously distributed.

The existence of a distribution of elementary microstructural mechanisms, which have individually an elastic perfectly-plastic behaviour, introduces the notion of discrete mem-

ory of particular events of the loading history, i.e. the inversion states. A clear manifestation of this discrete memory is made by the description of a small cycle inside a large cycle, which obviously shows the jump of the reference stress at the crossing of the preceding inversion state. The existence of this discrete memory appears surprising a priori, but becomes more understandable knowing that the material itself is its own support for this memory: it is the distribution of the internal stress of each microstructural mechanism which gives this memory. An easy topological representation of this stress distribution is done via the threshold of each mechanism and we verify that each load inversion state leaves a mark, in the shape of an angular discontinuity, in the internal stress distribution: this mark represents the memory of a past inversion state and this memory is of discrete type.

The pure hysteresis behaviour is one of the contributions of the mechanical behaviour of metallic materials. The pursuit of the qualitative analysis of the involved phenomena at the microscopic scale should allow us to suggest solutions for the other contributions of the behaviour global description. This may concern the definition of a physically relevant frame for expression of the stress rates, the description of viscosity effects, as well as taking of anisotropy into account.

Appendix. The symbolic model of pure hysteresis behaviour

The symbolic model of pure hysteresis behaviour has a strong heuristic character, at the macroscopic scale for the description of crystalline materials behaviour [25, 34, 23, 10] as well as at the microscopic scale for the interpretation of the microstructural mechanisms association (see Sec. 3, 4). In this appendix we analyse and briefly recall the model properties in view of helping to interprete experimental results obtained at both scales.

A.1. The definition of the symbolic model with springs and friction sliders

The model is composed of a parallel assembly of elements of different characteristic values. A single element is composed of the couple of a spring and a friction slider in series (Fig. 23a); its behaviour is defined by the spring rigidity G and the value for which the friction slider will move, which may be given by the load (or stress s) or the displacement (or strain e). The cyclic behaviour of a single element is elastic-perfectly plastic (Fig. 23a). The properties of an assembly of two elements is interesting in the sense that it shows some important points of the general behaviour (Fig. 23b), since locally the behaviour appears which is neither elastic nor perfectly plastic.

To obtain a model nearer real behaviour we have to consider a continuous distribution of elements (Fig. 23c), such that $g''(e)de$ is the rigidity of the elements comprised between e and $e+de$. For simplicity we admit that the function $g(e)$ is defined in the whole interval $[0, \infty]$, with the following limit values:

$$g''(0) = g'(0) = g(0) = 0 \quad \text{and} \quad g'''(0) > 0 .$$

Moreover we suppose that the total stress supported by the symbolic model has a finite value S_0:

$$S_0 = \int_0^\infty g''(e)ede .$$

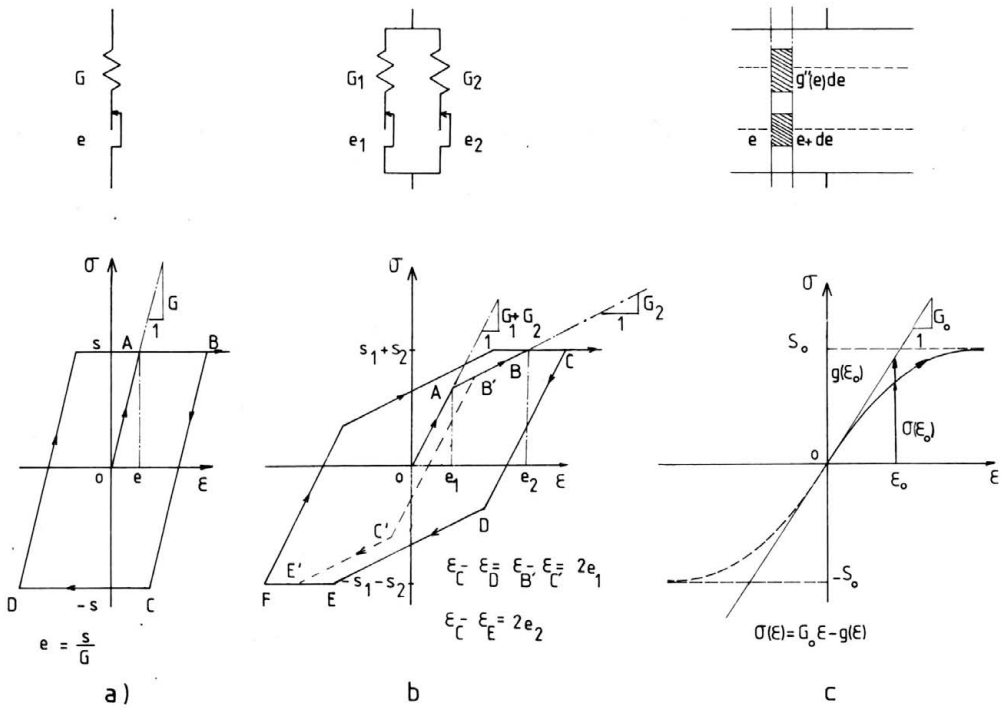

FIG. 23. The symbolic models.

Consequently, the first stress-strain loading branch is a smooth curve which admits for large strains a horizontal slope whose ordinate is S_0 and whose tangent at the origin is G_0:

$$G_0 = \int_0^\infty g''(e)de = g'(\infty).$$

By considering the stress contributions of the sliding elements and of the elements not sliding, we obtain:

$$\sigma(\varepsilon) = G_0\varepsilon - g(\varepsilon) = F(\varepsilon).$$

If we add a single spring, of rigidity $\hat{G}$, the model will admit for large strains a slope of value $\hat{G}$; the first loading branch is then written:

$$\sigma(\varepsilon) = (G_0 + \hat{G})\varepsilon - g(\varepsilon).$$

But in order to make more obvious the essential properties of the pure hysteresis behaviour, and to separate strictly the irreversible process from the reversible one, we consider in the following that $\hat{G}$ is zero, unless otherwise mentioned.

A.2. The topological diagram

The state of the model may be simply represented in a topological diagram: each couple of a spring and a friction slider is represented by a point whose abscissa is the

strain e for which the friction slider will move and the ordinate is the spring deformation ε_r. During loading the representative point will then move parallel to the ordinate axis along a straight segment comprised between the two bisectors $\varepsilon_r = \pm e$ (Fig. 24). The state of the model is represented by the line joining all the representative points. This line always terminates, on the large strain side, by a horizontal segment at $\varepsilon_r = cte$ representing all the couples whose slider never moves: this strain value is the model global strain ε.

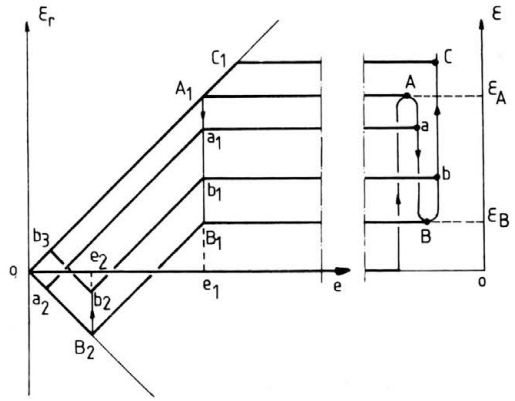

FIG. 24. The topological diagram.

Before any deformation takes place, the representative line of the model is the abscissa axis, since for each couple $\varepsilon_r = 0$. When the strain increases, the representative points shift equally, parallel to the ordinate axis, as long as the point is included in the angle of the two bisectors. When the representative point of a given couple reaches one of the bisectors this means that the corresponding friction slider moves ($\varepsilon_r = \epsilon$): then the representative point stays on the bisector as the global strain continues to increase. Thus after a first loading the representative line is OA_1A (Fig. 24). After an inversion all the sliders will stop sliding in that direction. The representative line will then shift as a whole in the reverse direction, the sliding beginning with the weaker couples: thus after the inversion the segment a_2a_1 stays parallel to the first bisector (Fig. 24).

A.3. The properties of the pure hysteresis model

In this subsection a description and an analysis of the properties of the pure hysteresis behaviour are given: it essentially concerns the mechanical aspects due to the possibility of experimental verification (see Sec. 2).

a. Since the strain limit of the weaker friction slider vanishes to zero, *the strain is irreversible however small it may be*: a friction slider will always move. Thus it is not necessary to introduce a separation between an elastic domain and a plastic domain.

b. Consider a path like OAB (Figs. 24 and 25); along path OA the friction sliders move progressively until the one characterized by threshold e_A. After the inversion at A, all friction sliders stop moving and tend to move in the reverse direction, starting with those of smaller threshold values. Thus *after an inversion the behaviour is locally restored*

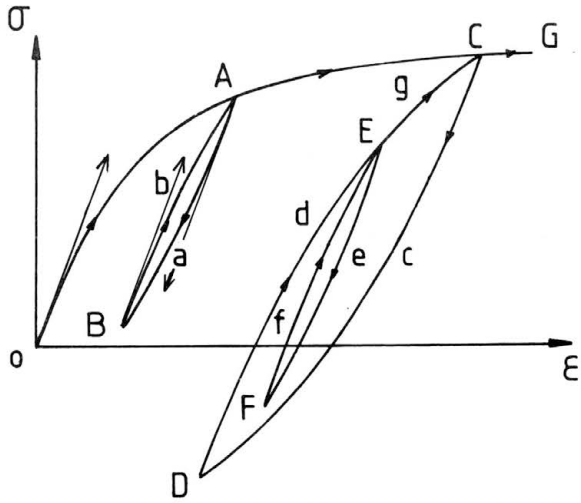

Path	ω	$_R\sigma$	$_R\varepsilon$	Branche	Arche
oA	1	0	0	1	1
AaB	2	σ_A	ε_A	2	1
BbA	2	σ_B	ε_B	3	1
AC	1	0	0	3	2
CcD	2	σ_C	ε_C	4	1
DdE	2	σ_D	ε_D	5	1
EeF	2	σ_E	ε_E	6	1
FfE	2	σ_F	ε_F	7	1
EgC	2	σ_D	ε_D	7	2
CG	1	0	0	7	3

FIG. 25. The principal properties of the pure hysteresis behaviour.

and the rigidity of the model is the same as at the origin:

$$\frac{d\sigma_{A^+}}{d\varepsilon} = G_0 .$$

c. Along the path AB a couple which previously moved for a deformation e_i now needs to be deformed by a value $2e_i$ before the friction slider moves in the opposite direction (Fig. 24). Thus the loading branch AB is similar, in the ratio 2, to the beginning of the first loading branch OA: this is the *Masing similarity rule* [25].

d. The restoration of the local behaviour after an inversion and the Masing similarity rule made conspicuous *the notion of discrete memory* of privileged states of the loading history: the inversion states. The behaviour is described by branches, or arcs of branches in more complex loadings, whose origin, called *reference state of the current branch*, is chosen between the preceding inversion states. Such unidimensional behaviour may be described by the following equation:

$$\sigma - {}_R\sigma = \omega F\left(\frac{\varepsilon - {}_R\varepsilon}{\omega}\right),$$

where the reference state coordinates ${}_R\varepsilon, {}_R\sigma$ and the similarity coefficient ω (or Masing coefficient) are piece-wise constant; a typical function is represented by a hyperbolic tangent:

$$\sigma - {}_R\sigma = \omega S_0 \operatorname{th}\left(\frac{2\mu}{S_0}\frac{\varepsilon - {}_R\varepsilon}{\omega}\right).$$

An example of complex cyclic loading is given in Fig. 25. One main intrinsic property of such behaviour is shown by branches like No 3 (or 7): the jump of the constants at the crossing of state A (or E and C) indicates that the model keeps the memory of particular events which are the preceding inversion states. After an inversion the representative line of the material state, in the topological diagram, is like Oa_2a_1a (Fig. 24). During the strain decrease the segment a_2a_1 stays parallel to the first bisector; the point a_2 moves continuously along the lower bisector; but the angle a_1 moves between the two bisectors by staying identical to itself. The existence of the segment a_2a_1 on one hand is the mark that some friction sliders have moved in the past. The existence of the angle a_1 on the other hand is the memory of the past inversion state A. This memory is not of viscous type, between current time and time t_A when the inversion happens, but a memory for which the model is its own support: the angle a_1 is an indelible mark which may be erased only in given conditions. This memory is of discrete type since there are only two alternatives for this mark: existence or nonexistence. Furthermore the erasure of this mark, and consequently of this memory, is possible under two conditions: first if the strain decrease is large enough so that the segment length a_2a_1 decreases to zero, secondly by making a second inversion in B and by increasing the strain farther than ε_A (arcs 1 and 2 of branch 3 of Fig. 25). The erasure of this memory results in a discontinuity in the stress-strain curve: in the first case it is a curvature discontinuity whereas in the second case it is a tangent discontinuity (Fig. 25).

The jump of the model rigidity between arcs 1 and 2 of branch 3 corresponds to the fact that when the segment b_3b_2 decreases to zero, the whole segment b_2b_1 reaches the upper bisector at the same time: this means that the point, which separates the friction sliders which move from the others, jumps from e_2 to e_1 (Fig. 24). In other words, during the loading BAC the characteristic strain interval of the moving friction sliders

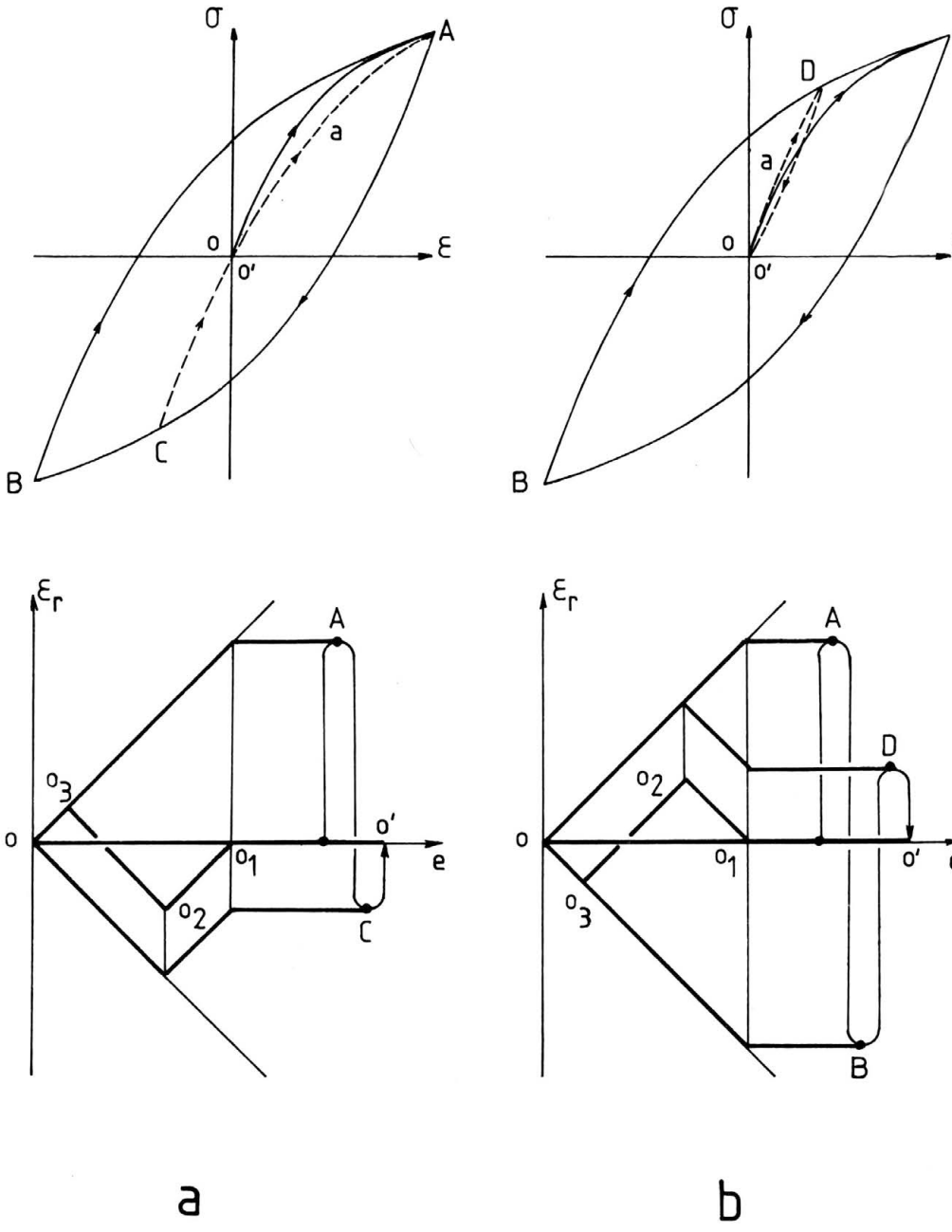

FIG. 26. Simple unloading to the origin.

is $[O, e_2 = \frac{1}{2}(\varepsilon_A - \varepsilon_B)]$ just before state A and $[O, e_1 = \varepsilon_A]$ just after state A. This discrete memory of inversion states will only exist in the case where the inversion really happens: thus there exists an essential difference between angles lying on the bisectors and the others, like the angle A_1 of state A and the angle a_1 of state a (Fig. 24). The latter

is the mark expressing at the current time the memory of inversion at state A which has occurred before; the former one is only a possible memory, but not yet revealed. Indeed, if we continue to increase the strain ε farther than ε_A, the angle will move farther along the bisector, ready to reveal a memory at higher strain.

e. This model of pure hysteresis behaviour possesses a *neutral state* which can be restored, whatever be the loading history. This statement seems a priori surprising since if an elastic material (spring) possesses a neutral state, it is not the case for a perfectly plastic material (friction slider). It is in fact the simple association of these elements which allows the existence of a neutral state, restorable in each and every case. This property is easily explained through the topological diagram. If we make a simple unloading towards the origin ($\varepsilon = \sigma = 0$) from point C or point D (Fig. 26), the representative line OO' of the model in the topological diagram is not a straight line, but a broken line whose angles materialize the memory of the preceding inversion states; thus the state O' does not represent the neutral state. This is confirmed by the reloading $O'aA$ or $O'aDA$, which differs from the first loading branch OA. To restore the neutral state it is necessary first to deform the model sufficiently in order to erase the memory of the preceding inversion states and bring the model state onto the first loading branch. Then a great number of almost symmetrical cycles of slowly decreasing amplitude must be made: this is the so-called fundamental cyclic test (Fig. 27). When the strain (and the stress) is zero, the representative line of the model state in the topological diagram is a "saw-toothed" line whose axis is the abscissa axis. The height of the teeth, directly related to the amplitude difference of two successive cycles, may be reduced at any desired value by increasing the number of cycles and making the broken line coincide with the horizontal line at the desired accuracy. After this restoration of the neutral state the reloading is identical to the first loading. Furthermore the locus described by the inversion points during the fundamental cyclic test is also identical to the first loading branch; this property is a direct consequence of the Masing similarity rule.

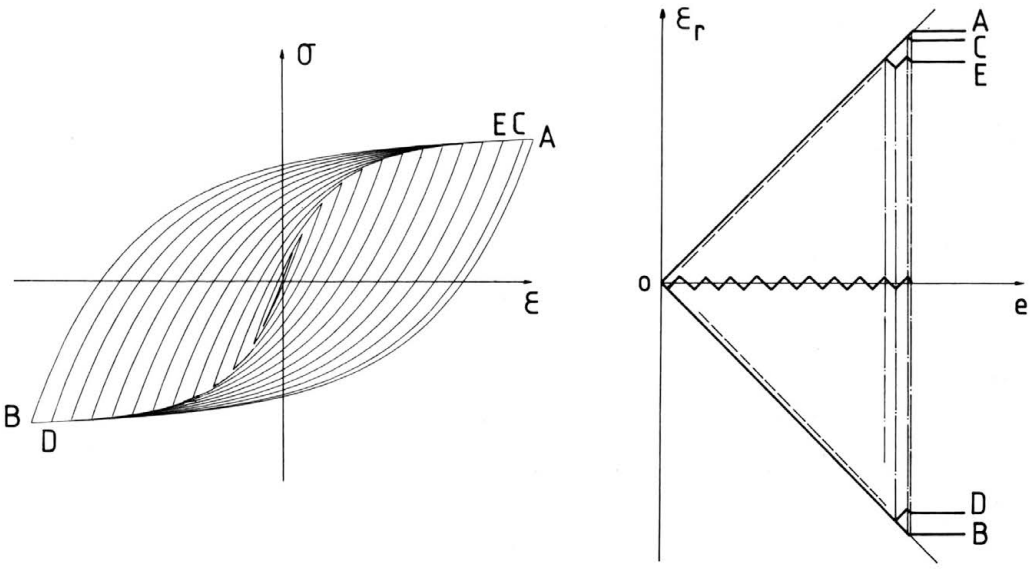

FIG. 27. The fundamental cyclic test.

A.4. Remarks

a. Concerning the *thermodynamical aspects*, we recall that the main point concerns the use of a reversible power π of discrete memory type [10]. In quasi-statical evolutions, which are only considered here, the energy balance may be written in the rate form:

$$P_e = \overset{\circ}{E} + (-\overset{\circ}{Q})$$

and by definition, the intrinsic dissipation ϕ is given by:

$$P_e = \phi + \pi ,$$

where P_e is the power of external forces, $\overset{\circ}{E}$ is the internal energy rate and $\overset{\circ}{Q}$ the heat rate associated with the internal irreversible phenomena; E is the energy stored by the springs and Q is the heat dissipated by the friction sliders.

Along the first loading, due to the immediate irreversibility of the strain, the intrinsic dissipation is taken equal to the power of external forces, i.e. the reversible power is then equal to zero. Immediately after an inversion, due to the quasi-elasticity of the behaviour, the intrinsic dissipation ϕ is zero and the reversible power π is equal to the power of the external forces. For simplicity and similarly to the first loading, it is supposed that the reversible power remains constant along the unloading branch. Thus the reversible power is written per arc of loading branch

$$\pi = {}_R\sigma \overset{\circ}{\varepsilon} ,$$

where ${}_R\sigma^*$ is the corresponding reference stress. The reversible power interferes in an equation of Gibbs type giving, from the thermodynamical point of view, the properties of the behaviour class considered here:

$$\overset{\circ}{E} = \overset{\circ}{I} + \pi ,$$

where $\overset{\circ}{I}$ is the disorder energy rate. Examples of the evolution of these rates are given in [10, 12, 14].

b. The pure hysteresis behaviour description is easy in the unidimensional case, since the definition of the piecewise constant is obvious. This is not the case in the general three-dimensional case: the solution is given by a correct thermodynamical interpretation of the model intuitive rules [10]. Thus the behaviour in the general case is described by a scheme composed of three main parts: a constitutive equation where piecewise constants interfere, an inversion criterion, which is nothing more other than the expression of the second law of thermodynamics, to detect the inversion states of the loading, and an algorithm to define at each moment the current value of the piecewise constants. This *constitutive scheme* makes conspicuous the coupling between the mechanical and the thermodynamical aspects of the behaviour. For more details see [10] or [11, 12].

c. As mentioned in Sec. 4, different types of assemblage for the springs and the friction sliders may be envisaged [23]. Between the simplest, the one considered here (Fig. 23) has the advantage of having an interpretation, equally for the single element and for the whole elements distribution. This assemblage is characterized by the fact that the total deformation is the same for all elements; consequently for a given total deformation there exists an internal stress distribution, associated with an internal plastic strain distribution.

d. The conditions given in Sec. A.1 did not define the shape of the loading branch, which may differ largely from one material to the other. The example given in Sec. A.3.d.

suggests a generalization in a differential form, the first loading branch being given by:

$$\frac{d\sigma}{d\varepsilon} = G_0\left[1 - \left(\frac{\sigma}{S_0}\right)^c\right].$$

By making the coefficient c vary in the interval $[0, \infty]$, the curve may cover, in the $\varepsilon - \sigma$ plane, all the domain defined by the abscissa axis, the tangent at the origin of slope G_0 and the asymptote of ordinate S_0. The preceding equation admits some analytical solutions; thus for $\varepsilon = S_0/G_0$ we have the following theoretical solutions for σ:

c	0	1	2	4	∞
σ/S_0	0	0.63	0.76	0.86	1

For real material the interval of interest for the coefficient c is $]1, \sim 4]$.

References

1. J.F. BELL, *The experimental foundation of solid mechanics*, Encyclopedia of Physics, **VI a/1**, Springer-Verlag, Berlin 1973.
2. E. HODKGINSON, *On the relative strength and other mechanical properties of cast iron obtained by hot and cold blast*, J. Franklin Inst., **24**, 184–196 and 238–257, 1839.
3. G. WERTHEIM, *Recherches sur l'élasticité*, Annales de Chimie et de Physique, third series, **12**, 385–454 and 581–610, 1844.
4. J. BAUSCHINGER, *Ueber die Quercontraction und Dilatation bei der Längenausdehnung and Zusammendrückung prismatischer Körper*, Civil Ingenieur, Leipzig, **25**, 81–124, 1879.
5. F.W. YOUNG, *On the yield stress of copper crystals*, J. Applied Phys., **33**, 963–969, 1962.
6. G. VELLAIKAL, *Some observations on microyielding in copper polycrystals*, Acta Metall., **17**, 1145–1154, 1969.
7. S.S. BRENNER, *Plastic deformation of copper and silver whiskers*, J. Appl. Phys., **28**, 1023–1026, 1957.
8. J.H. POYNTING, *On pressure perpendicular to the shear planes in finite pure shears and on the lengthening of loaded wires when twisted*, Proc. Roy. Soc. London, **A-82**, 546–559, 1909.
9. A. FOUX, *An experimental investigation of the Poynting effect*, Proc. Int. Symp. Second Order Effects, Haifa, 228–251, 1962.
10. P. GUELIN, *Remarques sur l'hystérésis mécanique*, J. Mecan., **19**, 217–247, 1980.
11. J.M. BOISSERIE, P. GUELIN, J.M. TERRIEZ, B. WACK, *Applications of a hereditary constitutive law of discrete memory type*, J. Eng. Mat. Tech., **105**, 155–161, 1983.
12. B. WACK, J.M. TERRIEZ, P. GUELIN, *A hereditary type, discrete memory, constitutive equation with applications to simple geometries*, Acta Mech., **50**, 9–37, 1983.
13. D. FAVIER, P. GUELIN, A. TOURABI, B. WACK and P. PEGON, *Ecrouissages — Schémas thermomécaniques et à variables internes: méthode de définition utilisant le concept d'hystérésis pure*, Arch. Mech., **40**, 611–640, 1988.
14. P. PEGON, *Contribution à l'étude de l'hystérésis elastoplastique*, Thesis, University of Grenoble, 1988.
15. D. FAVIER, *Contribution à l'étude théorique de l'élastohystérésis à température variable. Application aux propriétés de mémoire de forme*, Thesis, University of Grenoble, 1988.
16. S. HAN, *Le comportement d'hystérésis des solides et sa description par un schéma à mémoire discrète: le cas des aciers inoxydables*, Thesis, University of Grenoble, 1985.
17. S. HAN, B. WACK, *Properties of pure hysteresis behaviour of solids. Case of stainless steel and superalloy*, Arch. Mech., **38**, 439–462, 1986.
18. A. TOURABI, *Contribution à l'étude de l'hystérésis élastoplastique et de l'écrouissage de métaux et alliges réels*, Thesis, University of Grenoble, 1988.
19. F. LOUCHET, *Thermally activated dislocation sources in silicon*, J. Phys. C., Solid St. Phys., **13**, L847–L849, 1980.
20. J. COURBON, Private communication, 1989.
21. J. FRIEDEL, *Déformations finies des agrégats de métaux. Aspects physiques et métallurgiques*, Int. Symp. Physical Basis and Modelling of Finite Deformation of Aggregates, Paris, Sept. 30–Oct. 2, 1985.
22. U.F. KOCKS, A. ARGON, H. ASHBY, *Thermodynamics and kinetics of slip*, Prog. Met. Sc., 1975.
23. B. PERSOZ, *Modèles non linéaires*, La Rhéologie, 45–72, Masson, Paris, 1969.

24. H. BOUASSE, *Sur les déformations des corps solides*, Ann. de Chim. et de Phys., 7e série, **29**, 384–417, 1903.
25. G. MASING, *Zur Heyn'schen Theorie der Verfestigung der Metalle durch verborgene elastische Spannungen*, Wiss. Veroff. Siemens Konzern, **3**, 231–239, 1923.
26. J.F. BESSELING, *A theory of elastic, plastic, and creep deformations of an initially isotropic material showing anisotropic strain-hardening, creep recovery, and secondary creep*, J. Appl. Mech., **25**, 529–536, 1958.
27. H. MUGHRABI, *Dislocation wall and cell structures and long-range internal stresses in deformed metal crystals*, Acta Metall., **31**, 1367–1379, 1983.
28. C. HOLSTE, H.-J. BURMEISTER, *Change of long-range stresses in cyclic deformation*, Phys. Stal. Sol. (a), **57**, 269–280, 1980.
29. J. POLAK, M. KLESNIL, *The hysteresis loop 1, A statistical theory*, Fatigue Eng. Mat. Struct., **5**, 19–32, 1982.
30. H.-J. CHRIST, *Wechselverformung von Metallen*, Springer–Verlag, Berlin 1991.
31. W.E. DALBY, *Researches on the elastic properties and the plastic extension of metals*, Proc. Roy. Soc. London, **A-121**, 117–138, 1920.
32. E. KREMPL, *An experimental study of room-temperature rate sensitivity, creep and relaxation of AISI type 304 stainless steel*, J. Mech. Phys. Solids, **27**, 363–374, 1979.
33. D. MCLEAN, *Mechanical properties of metals*, Robert E. Krieger Publishing Company, Huntington (N.-Y.), 1977.
34. C. DE CARBON, *Déformation des solides*, Comp. Ren. Acad. Sc., **215-A**, 241–244, 1942.

LABORATOIRE DES SOLS, SOLIDES, STRUCTURES, GRENOBLE, FRANCE.

Received October 27, 1992.